Reviews

Activated Carbon Materials of Uniform Porosity from Polyaramid Fibers

S. Villar-Rodil, F. Suárez-García, J. I. Paredes, A. Martínez-Alonso, and J. M. D. Tascón*

Instituto Nacional del Carbón, CSIC, Apartado 73, 33080 Oviedo, Spain

Received June 22, 2005. Revised Manuscript Received August 18, 2005

Activated carbon fibers derived from polyaramids exhibit an outstandingly homogeneous pore size distribution. Here, we review the work carried out on the porosity characteristics of carbons prepared from these polymers, specifically Kevlar [poly(*p*-phenylene terephthalamide)] and Nomex [poly(*m*-phenylene isophthalamide)]. First, studies on the thermal decomposition of both polyaramid fibers and the reactivity of the resulting chars are reviewed in connection with the properties of the resulting products. Then, the porous texture of activated carbon fibers (ACFs) prepared by different methods (physical and chemical activation) is examined, with particular emphasis on the use of some novel methods to investigate microporosity in solids. Finally, the relationship between porosity and behavior of polyaramid-based carbons in several different types of application is analyzed.

1. Introduction: Why Polyaramids as Precursors for Porous Carbons?

Porous solids are an important class of materials with an ability to interact with atoms, molecules, and ions not only at their external surface but also throughout their internal surface.[1−4] Porous materials of a carbonaceous nature have a number of advantageous characteristics, such as very high surface area and pore volume, chemical inertness, and good mechanical stability.[1] Ideally, porous carbons should possess a homogeneous structure, with pores of uniform size and shape, so that thorough control of the properties and functionality of the material can be attained.[1,2] However, unlike other porous materials such as zeolites, the noncrystalline and complex structure of porous carbons has traditionally made such goal a difficult one to achieve.

Over the years, several different approaches for the control of the pore structure in carbons have been explored,[5] both at the micropore (pore size < 2 nm) and the mesopore (2−50 nm) level. Among them, the so-called template-based technique was found to be particularly suitable for the synthesis of carbons whose porosity is not only uniform in size and shape but also periodically ordered.[6−8] This approach has proved extremely successful for the synthesis of ordered mesoporous carbons,[9−17] which have shown good promise for several uses.[9,18,19] However, with regard to the synthesis of microporous carbons with uniform structure, the template-based technique has usually encountered important limitations, which can be mainly attributed to a deficient infiltration of the carbon precursor within the narrow channels of microporous templates.[6] For this reason, very few template-derived microporous carbons with a uniform, controlled structure are documented in the literature.[20,21] A recently reported alternative for the preparation of microporous carbons is centered in the extraction of metals from carbides.[22] Some of the resulting carbons display an outstandingly narrow pore size distribution (PSD) and are therefore considered to be good candidates for molecular sieving applications.

Another possibility for the synthesis of microporous carbons with uniform porosity, which is the one considered in the present review, is based on the well-known and relatively straightforward physical and chemical activation methods, but using highly crystalline organic precursors instead of materials with low or intermediate crystallinity that are typically employed for the preparation of activated carbons.[1] In this respect, work has mostly revolved around the use of polyaramid fibers as precursors since it was first reported that such highly ordered polymers were attractive materials for the production of activated carbon fibers (ACFs) with distinctive adsorption properties.[23−25] Several characteristics account for the interest of polyaramid-based ACFs, including their highly uniform microporous texture and high yields.

In this review, we provide a comprehensive account of the research that has been carried out on the development of porous carbons from highly ordered polyaramid fibers, specifically Kevlar [poly(*p*-phenylene terephthalamide)] and Nomex [poly(*m*-phenylene isophthalamide)] (registered trade names from DuPont, henceforth designated as Kevlar and Nomex). We focus on three main topics: (i) the thermal decomposition of the polymer fibers and the reactivity of the chars; (ii) the characterization of porosity in the resulting ACFs, placing special emphasis on the use of some novel methods for the investigation of microporosity in solids, and

* Corresponding author. Tel.: (+34) 985 11 90 90. Fax: (+34) 985 29 76 62. E-mail: tascon@incar.csic.es.

10.1021/cm051339t CCC: $30.25
Published on Web 10/11/2005

(iii) the relationship between porosity and applications of polyaramid-derived ACFs.

2. Studies on Pyrolysis of Polyaramid Fibers

The thermal decomposition or pyrolysis of polyaramid fibers is a relevant issue in connection with their application as fire-protecting materials[26] and their transformation into ACFs by either physical or chemical activation.[23−25,27−44] Early studies on Nomex and Kevlar pyrolysis were based on indirect information obtained from the analysis of their volatile degradation products.[45−49] Scarce evidence existed for the formation of carbon with isotropic, nongraphitizable structure (i.e., char),[50,51] a precondition to obtain microporous adsorbents by physical activation.[52] In this section, we review our current understanding of the pyrolysis of polyaramid fibers, paying particular attention to the studies of their solid residues.[53−58]

Scheme 1 shows the main stages in the transformation of Kevlar and Nomex into carbon fibers. Kevlar and Nomex only differ in the phenyl group linkage position: Kevlar is *para*-substituted, while Nomex is *meta*-substituted. However, this introduces important differences in the structure and properties of the corresponding fibers. Para substitution leads to increased rigidity along the polymer chain axis whereas meta substitution can introduce bends in the chains (see Scheme 1), which are detrimental to long-range order along the fiber axis and to the creation of an extended network of interchain hydrogen bonds. Furthermore, even in the most favorable case of pseudo-parallelism between chains, hydrogen bonding in Nomex is more impeded than in the case of Kevlar.

Thermoanalytical curves [simultaneous thermogravimetry (TG) and differential thermal analysis (DTA)] obtained under argon are shown in Figure 1. Nomex and Kevlar are chemically stable up to ca. 400[56] and 500 °C,[53] respectively. The only process taking place below these temperatures is the cleavage of the hydrogen bonds between polymeric chains (see Scheme 1), as verified by infrared spectroscopy of the solid residues.[53,56] Atomic force microscopy (AFM) showed that the polymeric chains loose their originally stretched arrangement to a small extent and the anisotropy of the starting material was only slightly reduced.[56]

The main process involved in the degradation of both polyaramids is the disruption of the polymeric chains to yield smaller units by the cleavage of amide bonds (see Scheme 1). However, Kevlar and Nomex differ in the reaction mechanisms: Heterolytic cleavage is feasible only for the meta isomer from 400 °C onward, while homolytic rupture takes place for both isomers in the 500−600 °C interval.[47,48] This is clearly reflected in the corresponding TG curves (see Figure 1): two main degradation steps are observed for Nomex (heterolytic and homolytic ruptures), whereas only one is found for Kevlar (homolytic rupture). As FT-IR results showed, the heterolytic cleavage leads to the appearance of carboxylic acids and primary amines, while the homolytic one mainly yields aryl nitriles.[53,56,58] The homolytic process is concurrent with the beginning of the condensation of the fragments into large polyaromatic compounds. Condensation continues at temperatures >600 °C, leading to carbonaceous materials with nanometer scale morphology typical of highly disorganized carbons, as observed by AFM and scanning tunneling microscopy (STM) (Figure 2).

The char yields on dry basis at 800 °C are approximately 36 wt % for Kevlar and 50 wt % for Nomex. Thus, the difference in the position of substitutions in the aromatic rings also introduces significant dissimilarities in the final yield. In general, the carbonization yield for the pyrolysis of any organic material is the result of two competing processes: bond cleavage and bond formation. Bond rupture leads to volatile loss, thus decreasing the yield, whereas bond formation occurs by condensation reactions and cross-linking. Therefore, any factor enhancing condensation or cross-linking will have a beneficial effect in the final yield. The para substitution in Kevlar leads to a linear, highly crystalline structure. Intuitively, this order must be detrimental to cross-linking, favoring the formation of volatile compounds by depolymerization reactions. This would explain the lower carbonization yield of Kevlar in relation to Nomex. Indeed, Yoon et al.[29,38] have succeeded to improve the yield of Kevlar pyrolysis (from 36 to 50 wt % at 800 °C) by adding an intermediate isothermal step at ∼410 °C, before the main degradation step takes place. This step favors the conversion of the linear aromatic chains to more condensed/cross-linked polyaromatic intermediates, which reduces the volatile loss in the subsequent heating to higher temperatures. However, Muñiz et al.[33] did not find such an improvement applying the same procedure.

Nomex pyrolysis in the presence of phosphoric acid, which is relevant to chemical activation with this agent, has also been studied.[58] Phosphoric acid promotes hydrolysis of the amide bond at low temperatures as well as an early generation of nitriles through a non-homolytic mechanism so that the degradation process of Nomex is shifted to lower temperatures. Besides, phosphoric acid favors cross-linking, leading to the early generation of chars and an increase in the char yield in relation to its nonimpregnated counterpart. Cross-linking reactions involve in this case the formation of phosphate and polyphosphate bridges between chains as well as the stabilization of a carbocation, which is an intermediate product of the main degradation reaction.

Elemental analyses of chars prepared from both polymers[31,56] indicated that there is an uncommon retention of heteroatoms (oxygen and, most of all, nitrogen) throughout the pyrolysis process. In fact, the limit established to consider a fiber as a carbon fiber (at least 92 wt % of the carbon element)[59] is not reached even at the highest temperature studied (960 °C). XPS studies of chars and ACFs prepared from Kevlar[60] have shown that nitrogen is present therein in chemically stable aromatic forms and that oxygen can be associated as well to the aromatic graphene network in pyridones or similar forms. The formation of stable polyaromatic structures containing heteroatoms during the pyrolysis process would explain their high retention in the chars. Oxygen can also be incorporated in hydroxyl or carboxylic forms as a consequence of exposure to ambient once the chars are cooled after their preparation.

As concerns the crystalline structure of chars from polyaramid pyrolysis, Cuesta et al.[60] reported, for Kevlar

Scheme 1. Main Stages in the Pyrolysis of Kevlar and Nomex Polyaramid Fibers

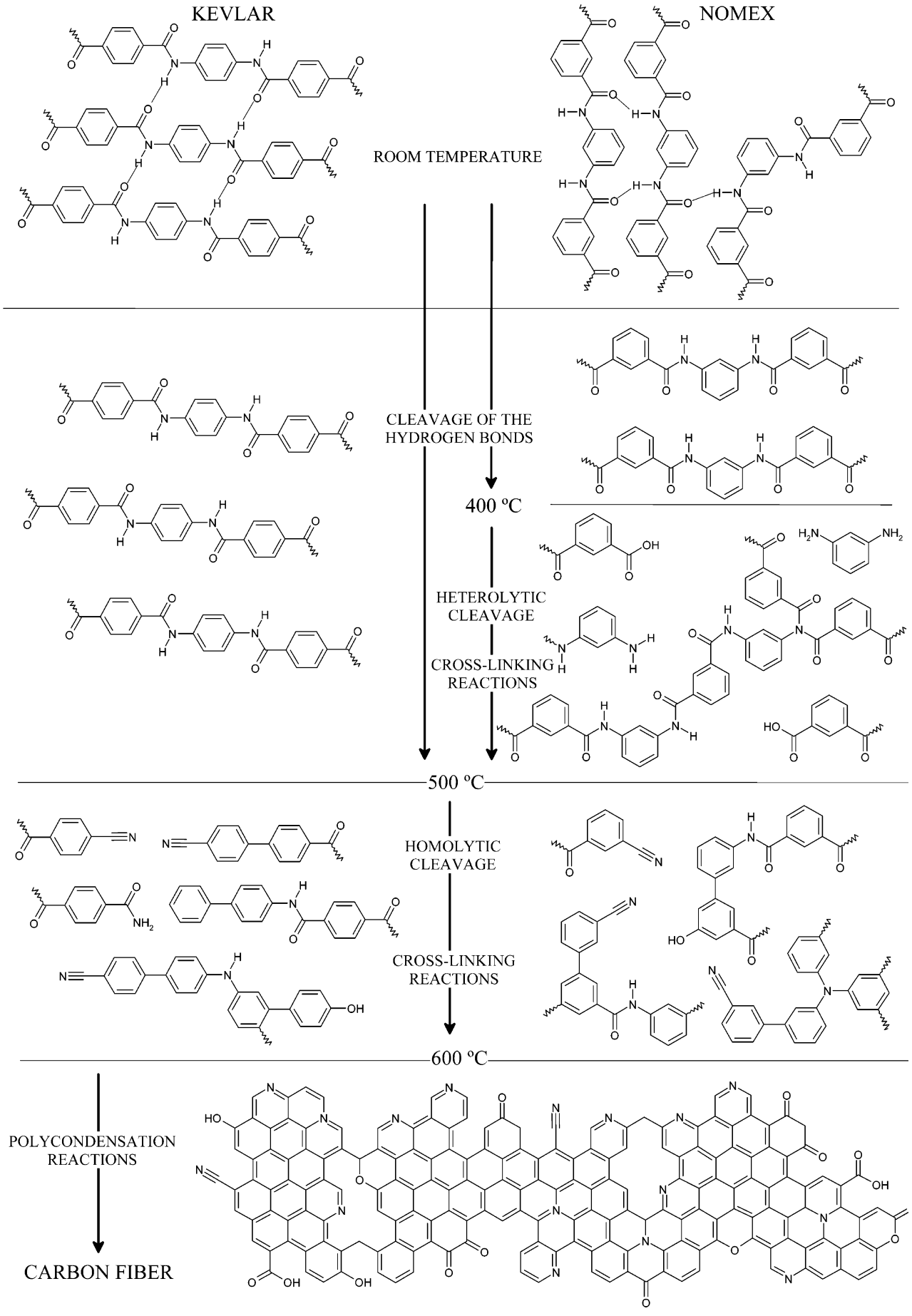

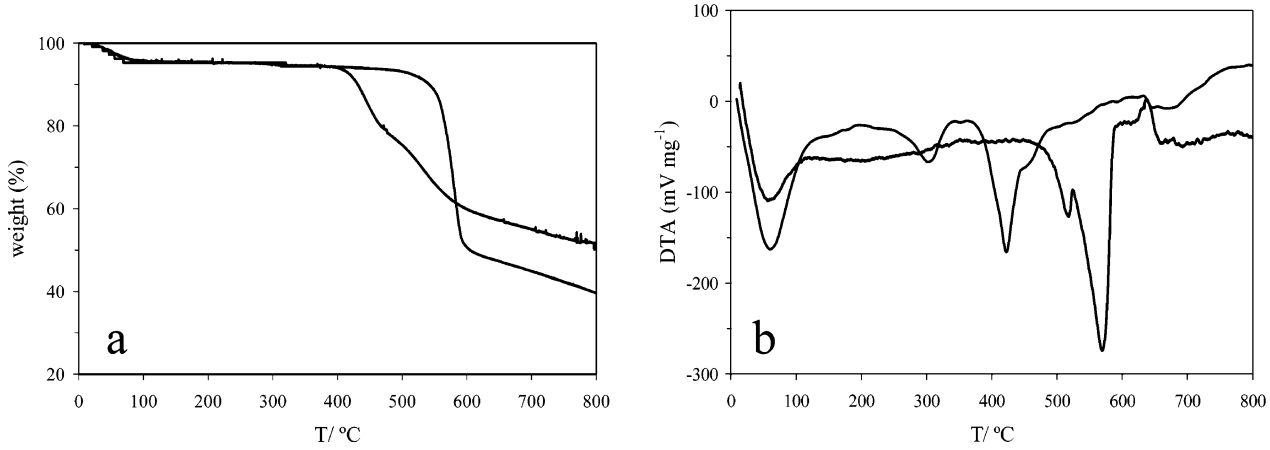

Figure 1. TG (a) and DTA (b) curves for Kevlar (thick lines) and Nomex (thin lines) pyrolysis. Adapted from refs 53 and 56.

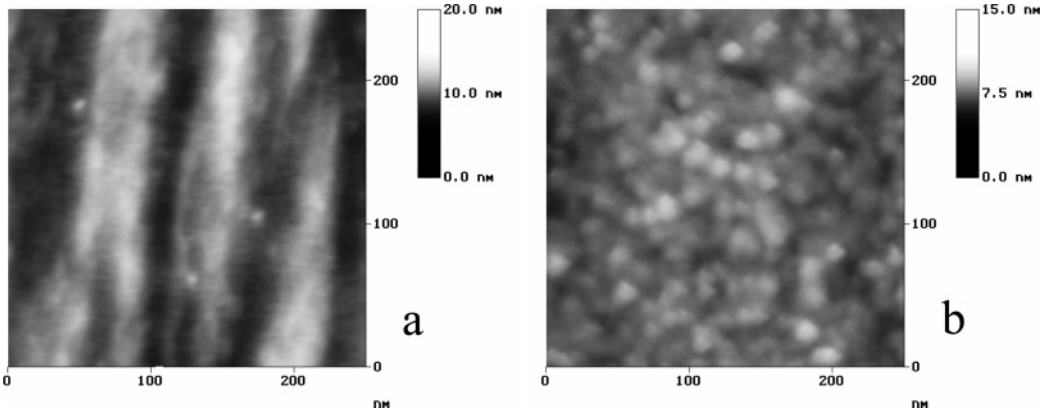

Figure 2. Typical nanometer-scale AFM images of (a) the starting Nomex fiber and (b) the carbon residue obtained following pyrolysis at 900 °C. Adapted from ref 56.

carbonized at 750 °C, values for the interlayer spacing (d_{002}) of 0.367 nm, height (L_c) of graphite-like crystallites of 2.3 nm, and width (L_a) of graphite-like crystallites of 7.2 nm. Accordingly, these chars are more ordered than chars and activated carbons obtained from conventional precursors such as coals or lignocellulosic feedstocks, and more ordered than isotropic carbon fibers.[61] Chars obtained from Nomex exhibited similar structural parameters to those of Kevlar chars. Thus, Nomex chars prepared at 850 °C yielded d_{002}, L_c, and L_a values of 0.372, 1.1, and 5.0 nm,[42] respectively, while those produced at 900 °C gave 0.365, 1.4, and 5.9 nm,[36] respectively. The crystal structure of Nomex chars is little dependent on the crystallinity of the precursor or the presence of carbon black as dye.[37]

As is the case of chars from other precursors, the porosity of solid residues from Kevlar and Nomex pyrolysis is rather incipient. Thus, nitrogen barely adsorbs on polyaramid-based chars, particularly those prepared from Nomex, whose apparent BET surface area (S_{BET}) was close to the geometrical surface area of the fibers. As is well-known, CO_2 at 0 °C is able to penetrate the network of narrow micropore solids.[62−64] Indeed, CO_2 adsorption pointed to an important development of narrow microporosity in both Kevlar and Nomex-derived chars.[65] Investigation of the effect of temperature on the evolution of microporosity of Nomex-based chars in the 550−900 °C range led to the choice of 800 °C as a convenient pyrolysis temperature, as it yields the char with maximum micropore volume.[65] Studies on the porosity of materials prepared by activation of these chars will be discussed in section 4.

3. Reactivity of Polyaramid Chars to Activation: Influence of Cross-linking

Nomex chars exhibit systematically lower gasification reactivity than Kevlar chars during physical activation.[24,30] Different factors are known to affect the reactivity of carbonaceous solids toward oxidizing gases. These factors can be classified into chemical, textural, and structural.[66] Generally speaking, an increase in the content of heteroatoms and inorganic impurities and/or in the surface area and porosity, and/or in the degree of structural disorder, will result in an enhancement in the oxidation reactivity of these materials.[66,67]

Chemical factors do not unequivocally explain the difference in reactivity. As indicated in section 2, chars from both polymers contain a high percentage of heteroatoms, and the differences in chemical composition are not large enough to explain the differences existing between the reaction rates of Kevlar and Nomex chars.[30] Tomlinson et al.[24] observed by SEM and energy-dispersive X-ray microanalysis (EDX) the occurrence of inorganic residues on the surfaces of chars and ACFs prepared from Kevlar and ascribed the differences in reactivity to these metal residues, which would act as gasification catalysts. Accordingly, other authors have identified the presence of Na_2SO_4 in Kevlar using both FT-IR[53] and AFM;[68] this was attributed to the fact that, in a step of fiber processing prior to spinning, sulfuric acid is used to

dissolve Kevlar to form an anisotropic liquid-crystal solution, the excess of H_2SO_4 being later neutralized with NaOH. The nonoccurrence of these two reagents in Nomex production would explain why virtually no inorganic impurities were found in Nomex-derived samples.[41,43] However, other authors[30,41,42,55,60] have not detected by SEM-EDX any residues on the surfaces of both Kevlar and Nomex chars.

Porous texture factors cannot justify either the observed trends. Although Martínez-Alonso et al.[31] and Cuesta et al.[60] showed that Kevlar chars exhibit an apparent BET surface area of 27 $m^2\ g^{-1}$ versus about 1 $m^2\ g^{-1}$ for Nomex chars as reported by different authors,[34,36,39−42] Stoeckli et al.[30] found lower immersion enthalpies for Kevlar chars than for Nomex chars; the low values of these enthalpies suggest a poorly developed or inaccessible porous structure in Kevlar chars.

As concerns the role of structural factors, as explained in section 2, both polymers lead to chars with similar crystal structures based on conventional XRD parameters (d_{002}, L_c, L_a). Therefore, from the average structural characteristics of Kevlar and Nomex chars, similar gasification reactivities would be predicted. However, it seems clear that the extent of cross-linking must play a key role in the reactivity of the chars. The crystallinity of polyaramid precursors is reflected in the ordered structure of the obtained chars ("memory effect"), which are formed by nanometer-sized crystals, as XRD studies showed. The position of substituents (meta or para) in the polyaramids influences the thermal degradation mechanism for both polymers, which is reflected in a higher yield in the case of Nomex due to the greater extent of cross-links among the nanocrystals generated during its degradation. Therefore, Kevlar chars will be formed by well-ordered regions (nanocrystals) mixed with other presumably more reactive areas where activation will take place preferentially. Unlike this, Nomex chars will exhibit a more uniform structure, formed principally by highly intermixed nanocrystals and with the presence of a few zones of high reactivity; therefore, in this case, gasification will take place more slowly and homogeneously.

No significant differences were found among the gasification rates of different varieties of Nomex.[37] Different degrees of crystallinity of the precursor polymer or the presence of carbon black as a dye do not have a significant effect on the degradation process itself and, thus, do not affect the extent of cross-linking, which seems to be the main parameter controlling the reactivity of the chars.

In preparing ACFs from Nomex pre-impregnated with small amounts of phosphoric acid (<9 wt %) by physical activation with CO_2 at 800 °C, Suárez-García et al.[41,42] observed that the use of this additive, besides increasing the carbonization yield as indicated in section 2, led to an increase in the gasification rate by more than an order of magnitude, which was associated with the presence of a greater amount of oxygenated functionalities in the chars from H_3PO_4-pre-impregnated Nomex.

4. Porosity Characterization of Polyaramid-Based Carbonaceous Materials

ACFs are usually prepared from low or intermediate crystallinity precursors such as viscose rayon or isotropic pitches.[69−71] Alternatively, Freeman et al.[23−25,27,28] first proposed the use of highly crystalline polyaramid fibers as precursors with the aim of obtaining ACFs with distinctive adsorption properties. Subsequently, various authors have prepared ACFs from Kevlar by physical activation with steam[23,24,30,32,33] or CO_2.[23,24,27,28,31,60] In the case of Nomex, activation has been carried out with steam,[24,25,30,32,33,35,39,40] with CO_2 using the polymer either alone[24,25,27,34,36,37] or pre-impregnated with small amounts of phosphoric acid,[41,42] or by chemical activation with phosphoric acid.[43,44]

The porous texture characterization of materials containing narrow micropores, such as the polyaramid-based ACFs under study, is not a trivial task as the standard adsorption measurements and theories suitable for most adsorbents are not applicable to solids with such small pore sizes. Due to the lack of a reliable procedure for the computation of the micropore size distribution from a single isotherm,[72] the use of a series of adsorptives varying in molecular size has been recommended as the best way to define the pore size in extremely microporous materials, such as carbon molecular sieves (CMSs).[73−76] Apart from the refined characterization of microporosity, the so-called molecular probe method provides supplementary information on the material's ability to adsorb pollutants such as volatile organic compounds (VOCs).[77,78] Immersion calorimetry can also be successfully applied to the characterization of activated carbons and CMSs.[79−87] Where more conventional methods fail, immersion calorimetry provides realistic values for the total surface area of ultramicroporous materials.[83] Likewise, as a complementary characterization technique, STM plays an important role by providing a direct visualization of these materials at the nanometer scale.[88] There are many examples in the literature on the application of STM to different types of porous carbons.[89−94] For polyaramid-based ACFs, the STM studies have afforded an understanding of the basic structures responsible for their special adsorption behavior.[42,95−97]

4.1. Carbon Fibers and ACFs Prepared from Kevlar and Nomex (Physical Activation). The ACFs obtained from Kevlar by physical activation, either with steam[28] or CO_2,[23,31] yielded N_2 adsorption isotherms of type I with a small contribution of type IV, as well as a small type H4 hysteresis loop that becomes more evident as the burnoff (BO) increases (see Figure 3). The adsorbents prepared at the lowest BOs exhibit low-pressure hysteresis (LPH), which remains evident even at the highest BOs in the samples activated with steam.[28] Occurrence of the LPH phenomenon is usually associated with either irreversible uptake of molecules in pores of about the same width as that of the adsorbate molecules and/or swelling of nonrigid pores.[79] In the present case, as LPH decreases or disappears as the BO increases, the first explanation is more plausible, indicating the presence of very narrow micropores with dimensions close to that of the N_2 molecules.

The different textural parameters calculated from the N_2 isotherms for Kevlar-derived materials go through a maximum at a BO near 60%, attaining apparent BET surface areas of 1000−1100 $m^2\ g^{-1}$, total pore volumes of 0.50 $cm^3\ g^{-1}$, and micropore volumes of 0.40 $cm^3\ g^{-1}$, an important fraction of which corresponds to ultramicropores (in this

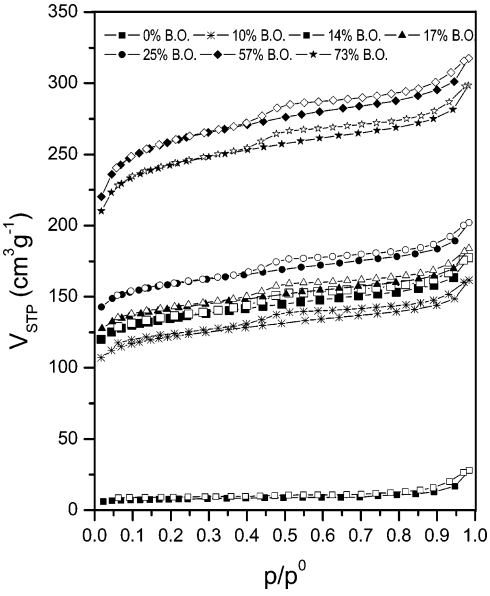

Figure 3. Representative nitrogen adsorption isotherms for CO_2-activated Kevlar chars at different BOs. Filled points, adsorption; empty points, desorption. Adapted from ref 31.

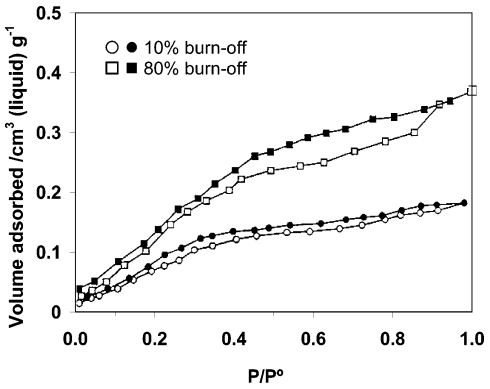

Figure 4. Water adsorption isotherms for ACFs derived from steam-activated Kevlar. Empty points, adsorption; filled points, desorption. Adapted from ref 23.

paper we will use this term with the meaning of "pores <0.7 nm in width"). Indeed, the micropore volumes and surfaces calculated from the isotherms of CO_2 at 0 °C are very close to those obtained from N_2 adsorption data (let us remind here that CO_2 at 0 °C and subatmospheric pressures only fills the narrowest micropores). On the other hand, the external surfaces of these samples are lower than 40 m^2 g^{-1}. These results indicate that the adsorbents prepared from Kevlar by physical activation are principally microporous, with a very scarce widening with increasing BO. It is to be mentioned that similar porous textural characteristics have been obtained with different varieties of Kevlar: either Kevlar pulp[31] or the more crystalline conventional Kevlar.[23,25,28] The decrease in porosity for the materials activated at BOs >60% has been associated with gasification-induced densification, whereby collapse or closure of pores occurs during activation and can compensate the possible creation of new pores by gasification.[23,31]

Figure 4 shows the water sorption isotherms measured at 25 °C on two ACFs prepared from Kevlar by steam activation to 10 and 80% BO. Both isotherms show a substantial uptake of water at low relative pressures, indicating possible interactions of the adsorbate with specific sites. Hysteresis is present throughout the whole relative pressure range. A characteristic early up-swing in Figure 4 extends up to a relative pressure of ∼0.3 (10% BO) or ∼0.5 (80% BO), and then the slope decreases. CO_2-activated Kevlar chars exhibited higher water uptakes,[23] but their behavior was qualitatively similar to those in Figure 4. The increase in water uptake at low relative pressures for the 80% BO chars relative to the 10% BO chars (which occurred with both activating agents) was attributed to a greater accessibility of hydrophilic sites rather than to a higher concentration of such sites, since the number of hydrophilic nitrogen sites decreased at high BOs. This low-pressure upswing was in clear contrast with findings with more conventional activated carbons, such as those obtained from rayon,[98] and led Freeman et al.[23] to conclude that peculiarities of water adsorption on polyaramid-based materials are not simply a matter of pore size, but they derive from a complex interrelationship between the effects of surface polarity, pore shape, and pore size.

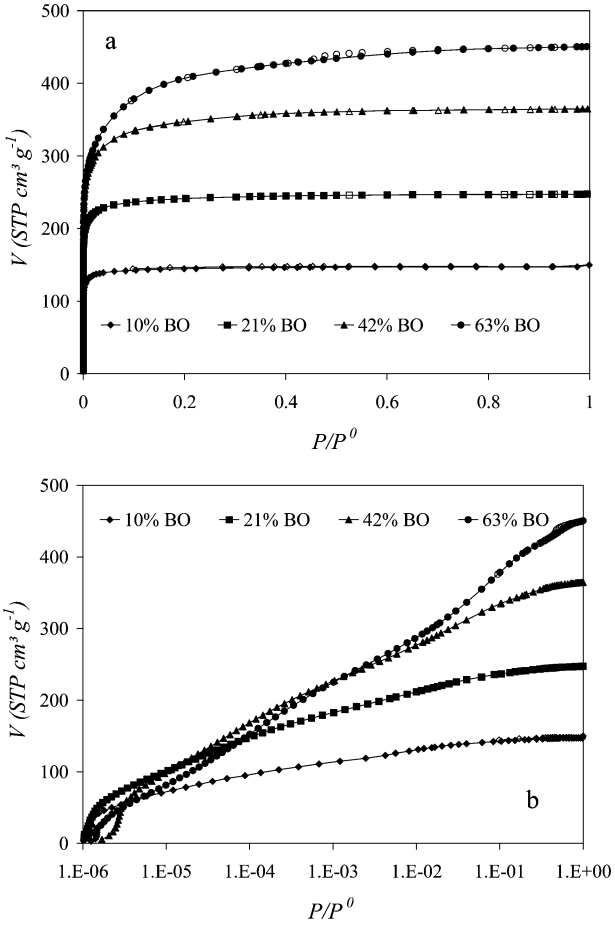

Figure 5. Representative nitrogen adsorption isotherms for steam-activated Nomex chars at different BOs in (a) conventional and (b) semilogarithmic scales. Filled points, adsorption; empty points, desorption. Adapted from ref 40.

ACFs prepared from Nomex by physical activation with steam[25,40] or CO_2[34,36,37] give rise to N_2 adsorption isotherms of type I, although distinctions can be established between them based on the widening of their knee as the BO increases. This can be seen in Figure 5, where for low BOs the isotherms are type Ia, which is indicative of the so-called

Table 1. Textural Parameters for a Series of Steam-Activated Nomex-Based Carbon Fibers[a]

% BO	S_{BET} ($m^2\ g^{-1}$)	$V_{p(N2)}$ ($cm^3\ g^{-1}$)	$V_{\mu p(DR,N2)}$ ($cm^3\ g^{-1}$)	$V_{\mu p(DR,CO2)}$ ($cm^3\ g^{-1}$)
0				0.16
10	560	0.23	0.23	0.22
21	936	0.38	0.38	0.26
42	1329	0.56	0.56	0.29
63	1580	0.69	0.68	0.38

[a] Adapted from ref 39.

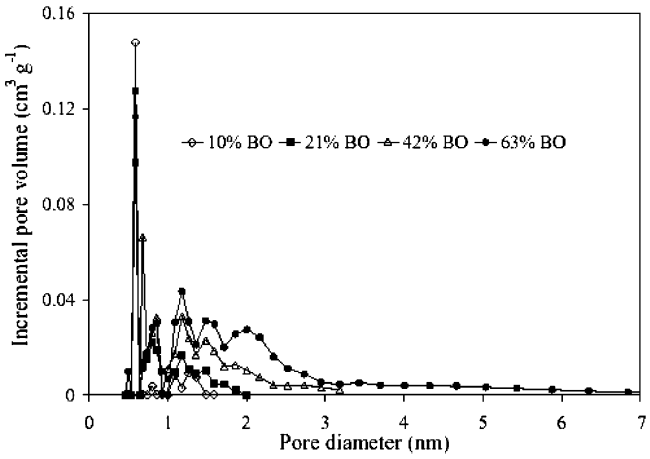

Figure 6. PSDs obtained for a series of ACFs prepared by steam activation of Nomex polyaramid fibers (at different BOs) from the N_2 adsorption isotherms through application of the NLDFT method. Adapted from ref 40.

primary micropore filling taking place at very low relative pressures in pores of molecular dimensions.[79] As the BO increases, a progressive widening of the isotherm "knee" occurs, changing to type Ib, where the N_2 uptake increases up to relative pressures of 0.2−0.3 (depending on the BO), indicating the presence of wide micropores that are filled by the so-called cooperative filling mechanism.[79] The materials prepared at the lowest BOs exhibit LPH which, as in the case of Kevlar, can be associated with the presence of pores with dimensions close to those of N_2 molecules. Textural parameters derived from N_2 and CO_2 adsorption are shown in Table 1. The chars and ACFs prepared at the lowest BOs exhibit micropore volumes calculated from the CO_2 isotherms higher than those obtained from the N_2 isotherms, which is characteristic for the presence of very narrow microporosity not accessible to N_2 due to activated diffusion.[99] As the BO increases, the micropore volumes calculated from N_2 become progressively larger than those from CO_2 adsorption, indicating a progressive widening of porosity; nevertheless, except for the highest BOs, the differences are small and the microporosity of these adsorbents has to be considered as relatively narrow and homogeneous. As Figure 6 shows, the PSDs [calculated by means of the nonlocal density functional theory (NLDFT)] of ACFs from Nomex are narrow and confined to the micropore/small mesopore (<3 nm) range, even for high BO degrees, exhibiting an important contribution of ultra-micropores, which makes these materials good candidates for use as molecular sieves.[40] This occurs even when the activating agent was steam, which, in comparison with CO_2, is well-known to produce a certain pore widening when using low or intermediate crystallinity precursors.[71]

A characteristic of ACFs obtained from Nomex is that all the textural parameters increase with increasing BO,[25,34,36,37,40] unlike the case of adsorbents prepared from Kevlar. Also, the porosity is less widened with increasing BO and the PSDs are narrower. This becomes evident by simply comparing the shapes of N_2 isotherms measured on ACFs from Kevlar and Nomex. Thus, the former (Figure 3) exhibit a certain slope at intermediate and high relative pressures as well as hysteresis, whereas the latter (Figure 5) are practically "rectangular", even for the samples prepared at high BOs. Therefore, Nomex-derived ACFs exhibit a narrower and more homogeneous porosity than equivalent materials prepared from Kevlar. This made it possible to prepare ACFs from Nomex with a porosity practically restricted to the micropore range (more than 90% of the pores being micropores) while exhibiting surface areas >2000 $m^2\ g^{-1}$ and pore volumes >1.1 $cm^3\ g^{-1}$.[42]

It seems convenient at this point to acknowledge that, in comparison with granular or powdered activated carbons, ACFs are already known to be essentially microporous with a rather homogeneous size.[100,101] In this context, Nomex-based ACFs would follow the general trend. However, a cursory comparison with results from the literature already shows that isotherms presented in Figure 5 exhibit a narrower "knee" than those for ACFs produced from either phenolic resins,[102] polyacrylonitrile,[103] acrylic textiles,[104] isotropic pitch,[105] or poly(vinyl chloride).[106] Moreover, some of these papers reported significant mesopore-related parameters, which were practically negligible in Figure 5 samples. Furthermore, as will be shown in section 4.4 and section 5.2, the fact that excellent carbon molecular sieves were obtained from Nomex-based ACFs confirms (indirectly) the fact that the latter had an outstandingly narrow PSD.

As in the aforementioned case of Kevlar, the use of Nomex varieties with different characteristics (degree of crystallization and incorporation or not of dyes) did not bring about appreciable differences in pore structure.[37] Accordingly, structural characteristics of the chars (obtained by X-ray diffraction) were independent of the variety of Nomex used. This is interesting from an economic point of view, as it allows using as feedstocks residues and/or byproducts from Nomex and Kevlar instead of the high-priced commercial varieties, without loss in textural properties of the resulting adsorbents.

Water adsorption isotherms at 25 °C on steam-activated ACFs from Nomex are shown in Figure 7a. The isotherm for the 10% BO material is almost entirely reversible and shows a gradual up-swing up to a relative pressure of ∼0.3, which is followed by a plateau. In contrast, the isotherm for the 80% BO ACF is very similar to those obtained for many commercial activated carbons. The material prepared by CO_2 activation to 10% BO of Nomex char yielded an isotherm (Figure 7b) similar in shape to that for the 10% BO steam-activated one, whereas the material prepared by CO_2 activation to 80% BO gave an isotherm (Figure 7b) intermediate in shape between those shown in Figure 7a, with a narrow hysteresis loop that extended throughout the whole relative pressure range.[25] As in the aforementioned case of Kevlar, the early upswing at 10% BO can be attributed to the

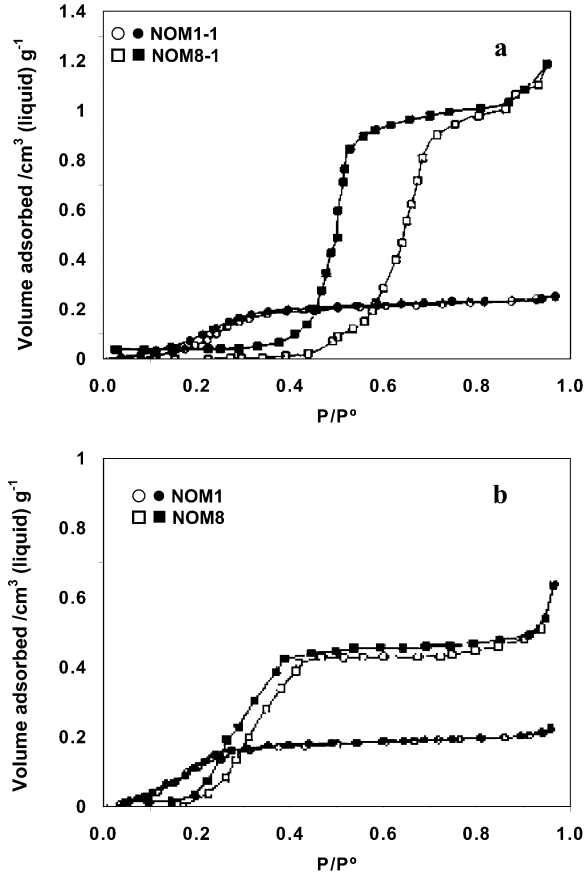

Figure 7. Water adsorption isotherms for ACFs derived from steam-activated (a) and CO_2-activated (b) Nomex chars. Empty points, adsorption; filled points, desorption. NOM1-1 and NOM8-1 in (a) stand for Nomex chars steam-activated to 10 and 80% BO, respectively. NOM1 and NOM8 in (b) were activated in CO_2 at the same BOs. Adapted from ref 25.

presence of specific sites for adsorption, likely nitrogen residues. However, the relative hydrophobicity at low relative pressures for the two materials activated at 80% BO could not be simply ascribed to loss of such polar sites, as nitrogen content was almost identical to that of the 10% BO material. This led Freeman et al.[25] to assume that different types of nitrogen sites with different accessibility must exist in these Nomex-derived ACFs.

The refined characterization of the porous texture of ACFs derived from Kevlar and Nomex by the following techniques confirms and completes the results obtained by physical adsorption of gases, evidencing the high adsorption capacities and the particularly narrow and homogeneous porosity of these adsorbents, independently of the variety of feedstock and the activation method used. Immersion calorimetry into different liquids of nonactivated and steam-activated carbon fibers derived from Kevlar and Nomex was done by Stoeckli et al.[30] Their results corroborated that, unlike usual findings for ACFs derived from low-crystallinity precursors,[107−110] steam activation of polyaramid fibers leads to materials similar to those obtained by carbon dioxide activation. Indeed, steam-activation of polyaramid-based carbon fibers yielded adsorbents not only with a large adsorption capacity but also with narrow pores. These features, together with their fibrous morphology, make such activated carbons very selective adsorbents, potentially useful for gas separation processes. In fact, the detailed characterization of a series of steam-activated Nomex-derived ACFs through immersion calorimetry into dichloromethane, benzene, and cyclohexane[39,40] and adsorption of the corresponding vapors[111] revealed a significant adsorption selectivity. Indeed, the char and the ACFs activated to low BOs showed molecular sieving behavior for dichloromethane/benzene; the ACFs activated to intermediate BOs possessed molecular sieve effects for the couples dichloromethane/cyclohexane and benzene/cyclohexane; finally, the ACFs activated to higher BOs possessed high capacity for any of the three aforementioned substances and could be in principle good adsorbents for such pollutants in air.

It was shown by STM that, irrespective of the different specific conditions of activation investigated for crystalline Nomex, the nanometer-scale structure of all the activated materials prepared thereof was extremely homogeneous and always followed the same general pattern:[42,96,97] a close-packed arrangement of carbon platelets with typical lateral dimensions of a few to several nanometers and an interconnected network of narrow channels (slits) between the platelets, that corresponds to the porous system of the carbons (e.g., Figure 8, a and b). The channel widths measured by STM were quite uniform, and although some variation in the typical ranges were reported for different samples, in all cases the values lay within the micropore range and mesoporosity was practically absent, in agreement with the gas adsorption results.[42,96,97] It could therefore be concluded that such a highly uniform nanostructure provided the basis for the outstanding homogeneity in pore size of the Nomex-based ACFs and their remarkable adsorption characteristics. By contrast, STM indicated that the use of low crystallinity precursors (e.g., phenolic resin, coconut shell, or cellulose) resulted in activated carbons of heterogeneous nanostructure, with micro- and mesopores of considerably varied sizes, and where the porous texture did not display the continuous, interconnected network obtained when Nomex was used as a precursor,[89−92] as illustrated in Figure 8c for a phenolic resin-derived activated carbon. Kevlar-derived ACFs were also investigated by STM.[95] In this case, the pore structure was dominated by micropores, but some spongy mesoporous areas were also observed. The micropores were mainly of slit type and about 1 nm wide, whereas the mesopore sizes ranged from 4 to 16 nm. These pore sizes determined by STM were in agreement with those deduced from gas adsorption data for the Kevlar-derived ACFs.[31,95]

The fibrous shape of ACFs facilitates the preparation of consolidated forms. Indeed, low-density Nomex rejects-based ACF composites were prepared by dry-mixing Nomex rejects carbonized at 850 °C with powdered phenolic resin in a mass ratio 3/1.[35] The mixture was cured at 180 °C and carbonized at 700 °C, yielding a material with bulk density of ∼0.25 g cm^{-3}. The obtained ACF monoliths (ACFMs) were steam-activated at 700 °C to different BO degrees. The textural characteristics of the resulting materials, evaluated by both CO_2 and N_2 adsorption, are similar to those reported for loose activated Nomex-based ACFs. Different authors[112,113] have observed an unusual crossover in *n*-butane adsorption capacity of ACFs: At *n*-butane concentrations above ∼5000 ppm the adsorption capacity is proportional to the S_{BET}, but the

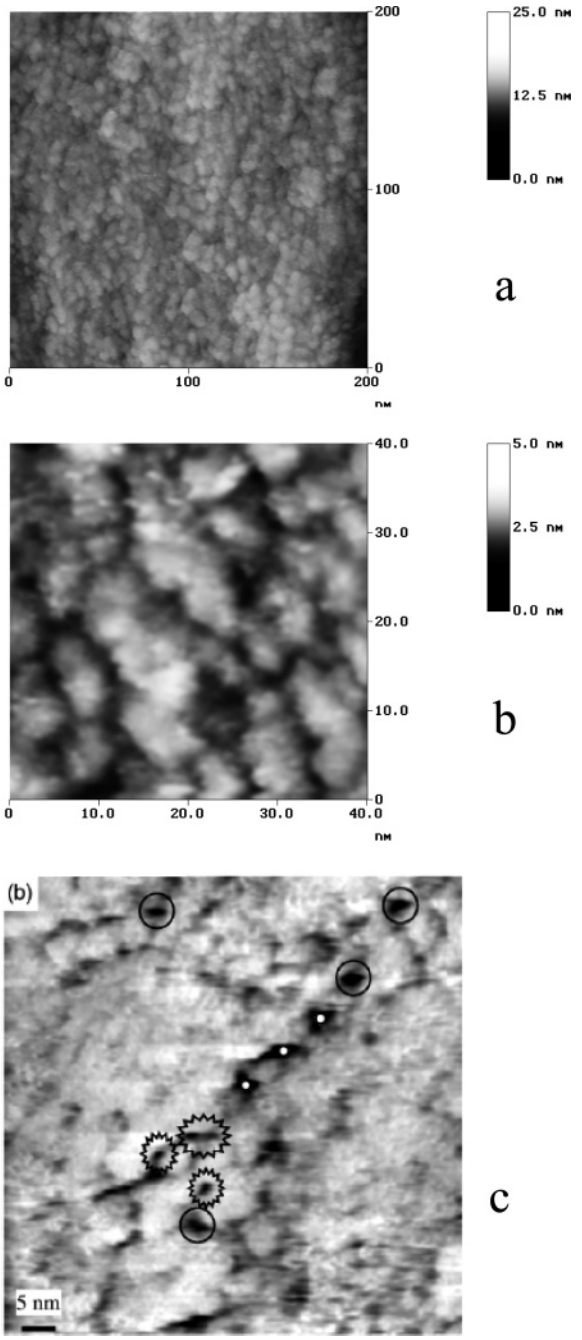

Figure 8. Nanometer-scale STM images of ultra-high surface area carbon fiber prepared by CO_2 activation of Nomex pre-impregnated with H_3PO_4. (a) General appearance. (b) Detailed image showing extensive networks of 2−3 nm wide pores. Included for comparison is an STM image of a porous carbon prepared by activation of phenolic resin spheres (c). The pores (denoted by circles, stars, and dots) do not form highly interconnected networks as in (b). Adapted from refs 42 (a and b) and 92 (c).

trend was reversed for lower concentrations.[112] The previously described ACF composites were used to analyze the correlation between the crossover phenomenon and the micropore size distribution of the ACFs,[114] which was assessed by immersion calorimetry into different liquids. At high adsorptive concentrations, when the entire micropore system is involved in the adsorption process, the adsorption capacity was found to be directly related to the total pore volume. On the other hand, the micropore size distribution determined the adsorption capacity at low concentrations.

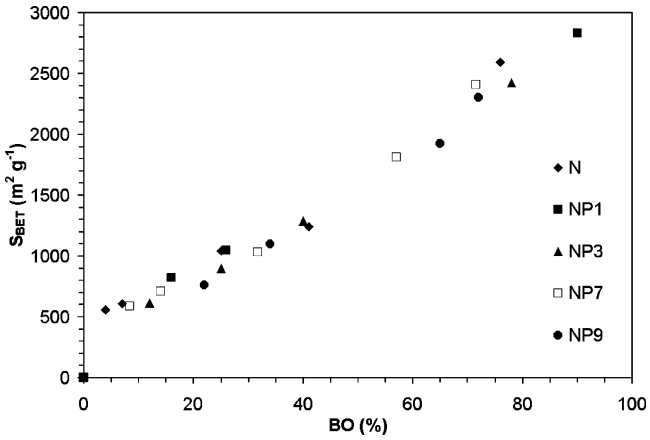

Figure 9. Evolution in the apparent BET surface area with the BO degree for various series of samples prepared by physical activation with CO_2 from Nomex, either alone (N series) or pre-impregnated with different amounts of phosphoric acid (NP series, where the number that follows: 1, 3, 7, or 9, indicates the impregnation ratio in wt % H_3PO_4 relative to Nomex precursor). Adapted from ref 42.

4.2. Nomex-Derived ACFs (Pre-impregnated Samples + Physical Activation). In preparing ACFs from Nomex pre-impregnated with small amounts of phosphoric acid (<9 wt %) by physical activation with CO_2 at 800 °C, Suárez-García et al.[41,42] have observed that this additive has two beneficial effects on Nomex pyrolysis-activation: (i) an increase in char yield (by more than 12% for an amount of H_3PO_4 of 9 wt %) and (ii) an increase in gasification reactivity by more than 1 order of magnitude. The increase in yield was associated with a change in the mechanism of thermal degradation of Nomex in the pyrolysis step that lends a decrease in volatile evolution, with a corresponding increase in char yield.[58] The increase in gasification rate was associated with the presence of a larger amount of oxygenated functionalities in the chars.

The porous textural characterization by gas physisorption of ACFs obtained from fresh or pre-impregnated Nomex reveals that the H_3PO_4 additive does not affect the porous texture of these adsorbents. Thus, Figure 9 shows the evolution in the apparent BET surface area with the BO degree for various series of samples prepared by physical activation with CO_2 from Nomex, either alone (N series) or pre-impregnated with different amounts of phosphoric acid (NP series, where the number 1, 3, 7, or 9 indicates the impregnation ratio in wt %). The surface area increases practically linearly with increasing BO degree and is not affected by the amount of phosphoric acid. The ACFs obtained by this procedure exhibited the same behavior as indicated in section 4.1 for physically activated Nomex: the porosity increased with increasing BO degree, but remained restricted to the micropore size. N_2 adsorption isotherms of type Ia were obtained for BOs < 50%, which changed to type Ib for BO > 50%.[42] The ACFs prepared at the highest BOs (>70%) exhibited surface areas >2000 m^2 g^{-1}, total pore volumes > 1.10 cm^3 g^{-1}, and micropore volumes >1.00 cm^3 g^{-1}. The PSDs exhibited a slight increase in pore size with increasing BO, but remaining restricted to the micropore/ small mesopore region (no pores >3−4 nm were found, even for the ACFs with ultrahigh surface area prepared at the highest BOs).

The characterization of the microporosity of these materials was further refined by measurements of the adsorption of vapors with different molecular sizes (benzene, *n*-hexane, cyclohexane, and 2,2-dimethylbutane).[115] Significant molecular sieve effects were found for the couples benzene/cyclohexane and *n*-hexane/cyclohexane for all the materials in the series of ACFs. The fact that these effects were found irrespective of the BO degree indicates that the pore width is remarkably constant throughout the activation process. From the molecular sizes of the probe molecules[116] a proximate pore width of 0.6 nm could be established. This agrees with the PSDs obtained by NLDFT from gas adsorption results.

As mentioned previously, STM investigations revealed that the nanostructure of all ACFs prepared from crystalline Nomex consisted of a highly uniform platelet ensemble, which in turn defined the porous framework of these carbons. For the ultrahigh surface area fibers prepared from preimpregnated Nomex, the platelets were quite small (2−5 nm), while the micropores were relatively wide (1.5−2.5 nm) and particularly well interconnected (Figure 8a,b),[42] in contrast to the case of the non-superactivated material.[96,97] This suggested that the slight pore widening took place by eroding the carbon platelets, as expected for activations based on gasification. Furthermore, the micropore sizes measured by STM compared favorably with those deduced from N_2 adsorption data, and the very high adsorptive capability of these materials could be attributed to the dense porous network that was formed.

4.3. Nomex-Derived ACFs (Chemical Activation). Phosphoric acid is one of the most often used agents for the preparation of carbon adsorbents by chemical activation of precursors such as coals[117,118] and, especially, lignocellulosic materials.[119−123] Phosphoric acid activation of Nomex fibers[43,44] represented the first preparation of ACFs by this method from a noncellulosic fibrous polymer. The amount of phosphoric acid employed had a strong effect on the porosity developed. Suárez-García et al.[43] showed that the N_2 isotherms changed from type Ia for impregnation ratios <106 wt % to type Ib for greater amounts of H_3PO_4. Porosity development was maximal in the temperature interval in which thermal degradation of Nomex takes place in the presence of phosphoric acid (400−500 °C).[44,58] Phosphoric acid activation of other precursors usually leads to mesoporous carbons at high impregnation ratios.[117−123] However, essentially microporous carbons are obtained from Nomex even at high impregnation ratios. The corresponding PSDs, calculated by the NLDFT method, are shown in Figure 10. It can be seen that ultra-micropores strongly contribute to the porosity, and that no pores >3 nm in width are present, even at the largest impregnation ratios. Consequently, a "memory effect" is again found in chemical activation with phosphoric acid.

4.4. Nomex-Derived ACFs Modified through CVD Treatments. In an aim to obtain materials with uniform and narrow porosity, the porous texture of Nomex-derived ACFs was modified by chemical vapor deposition (CVD) of benzene[124] and methane.[97] The CVD treatment led to a strong decrease in N_2 uptake, which was accompanied by the appearance of LPH; for the longest CVD treatments, N_2 adsorption became negligible. On the other hand, CO_2 adsorption did not decrease to a great extent with increasing CVD time. A slight decrease in the micropore volume calculated from CO_2 adsorption was observed in the first stages of the treatment, while after a certain CVD time this value remained constant, indicating that the narrowest microporosity was kept along with the CVD process. A comparison of the evolution in uptake of N_2 and CO_2 during the CVD treatments allows one to conclude that carbon deposition took place in the correct way; i.e., it occurred preferentially at the pore mouths, thus lending a progressive decrease in pore size without loss in pore volume. Therefore, materials with both narrow PSDs and high adsorption capacities were obtained.

Measurements of adsorption of vapors with different molecular sizes (dichloromethane, benzene, and cyclohexane) and immersion microcalorimetry using the corresponding liquids allowed refinement of the evolution of porosity during the CVD process on Nomex-derived ACFs and characterization of the size exclusion properties of the obtained materials.[97,111,125,126] The results are given jointly in Table 2, where the samples are designated as follows: Bz/Mt indicates that the CVD treatment has been done with benzene or methane, respectively; the first number is the concentration of the organic species in the gas flow and the second one is the CVD treatment time in minutes (for example, Mt 100-10

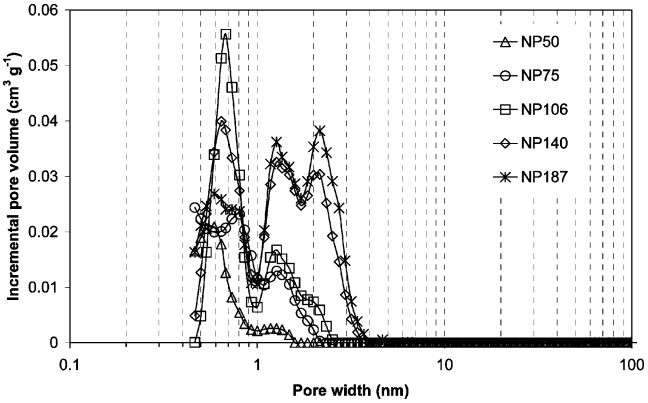

Figure 10. PSDs obtained for a series of ACFs prepared by chemical activation with H_3PO_4 of Nomex polyaramid fibers from the N_2 adsorption isotherms through application of the NLDFT method. Sample reference codes: as in Figure 9. Adapted from ref 43.

Table 2. Total Pore Volumes Derived from the Adsorption of Different Vapors at 298 K and Specific Surface Areas Derived from the Experimental Enthalpies of Immersion into the Corresponding Liquids at the Same Temperature for Materials Prepared by CVD of Benzene (Bz) and Methane (Mt) on Nomex-Derived ACFs Activated to 21% BO[a]

	total pore volume (cm^3 g^{-1})			specific surface areas (m^2 g^{-1})		
samples	CH_2Cl_2	C_6H_6	C_6H_{12}	CH_2Cl_2	C_6H_6	C_6H_{12}
Bz 3-120	0.27	0.26	0.01	899	923	189
Bz 3-180	0.23	0.02	0.01	698	121	52
Mt 100-10	0.27	0.27	0.04	919	876	93
Mt 100-20	0.13	0.04	0.02	143	109	74
Mt 23-45	0.15	0.01	0.01	393	108	34
Mt 23-60	0.09	0.01	0.01	99	115	59

[a] The first number indicates the concentration of the organic species in the gas flow, and the second is the CVD treatment time in minutes. Adapted from ref 97.

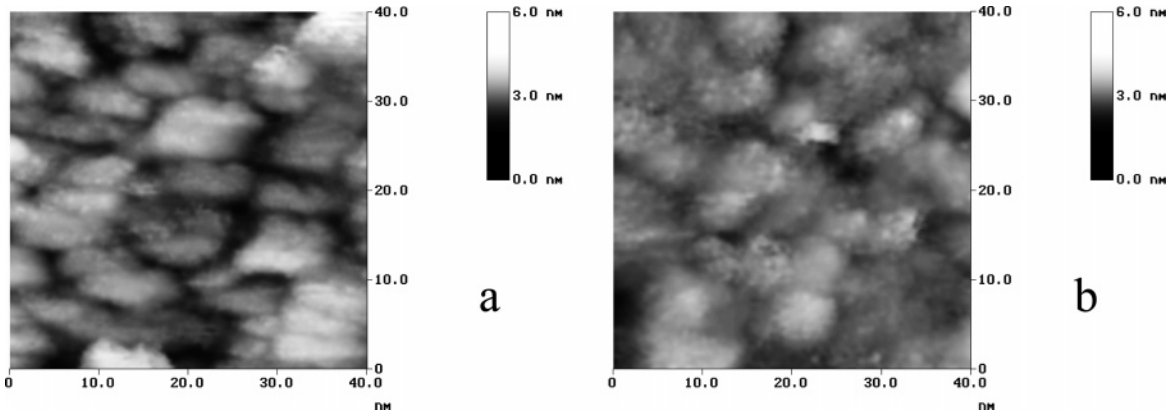

Figure 11. Nanometer-scale STM images of a Nomex-based steam-activated carbon fiber (a) before and (b) after CVD treatment of benzene to obtain a carbon molecular sieve. Adapted from ref 96.

stands for a material CVD-treated with a pure stream of methane for 10 min). Both the immersion microcalorimetry and the vapor adsorption results confirm that the CVD treatments succeeded in narrowing the pore mouths so as to restrict the entrance of the bigger molecules (benzene and cyclohexane), putting forward higher selectivity while preserving a good adsorption capacity that is reflected in the admittance of dichloromethane.[97,111,125] Furthermore, these techniques were able to detect subtle differences in the porous textures of the materials obtained through CVD of benzene[111,125,126] and methane,[97] indicating that the closure of the pore mouths when using the latter gas had gone further than with the former.

STM was successfully employed to disclose the structural changes undergone by the steam- or CO_2-activated Nomex-derived material upon CVD treatment.[96,97] Specifically, pore mouth narrowing after the carbon deposition could be directly visualized by this technique. For instance, the nanostructure of the original steam-activated fibers was comprised of 4−10 nm large platelets and 0.7−1.5 nm wide pores (Figure 11a). Following CVD of benzene, the platelet arrangement was still apparent in the STM images, but the channels became noticeably (and homogeneously) narrower (down to 0.6−0.7 nm), indicating that good control over the deposition could be achieved in this case, as carbon was deposited only on the pore mouths and not on the fiber external surface (Figure 11b).[96] By contrast, evidence of external deposits of pyrolytic carbon that buried most of the platelets was found in the case of CMSs prepared by CVD of methane, and the number of channels was considerably reduced in relation to that of the starting ACFs.[97]

5. Relationship between Pore Size Control and Applications of Polyaramid-Derived Carbons

Activated carbons are typically used as adsorbents, catalysts, or catalyst supports in environmental control. ACFs can actually be used for any application of the more conventional activated carbon granulates or powders but they offer a number of advantages over them. Their high internal surfaces and small fiber diameter bring about low mass-transfer resistance and fast adsorption kinetics. Besides, their fibrous shape facilitates the preparation of consolidated forms (felts, fabrics, and monoliths). The main drawback for their use in industry is their high price. However, the use as feedstock material of low-quality fibers rejected from the manufacture process of the polymeric fiber can help to keep the process feasible from an economic point of view. These rejects do not meet the appropriate mechanical properties for their commercialization as high-performance polymeric fibers, but they are still chemically and morphologically equivalent to the commercial fibers and thus suitable for production of ACFs. In this context, Kevlar and Nomex low-quality rejects as well as the first-grade materials have been used as precursors for ACFs with different targets.

5.1. Environmental Applications. Acid rain is related to nitrogen and sulfur oxides (NO_x and SO_x), whereas CO, NO_x, particulates, and volatile organic compounds (VOCs) are implied in smog formation. Activated carbons have been used in different ways for the removal of these pollutants. Polyaramid-derived ACFs have shown to be especially effective due to their special porous texture and surface chemistry.

5.1.1. VOCs Removal. Nomex-derived ACFs have been tested as adsorbents for the retention of VOCs. As explained at the end of section 4.1, at low concentrations such as the ones found in realistic polluted environments, the amount adsorbed mainly depends on the PSD of the adsorbent and, particularly, on the amount of narrow micropores.[114] Indeed, Nomex-based ACFMs have been shown to adsorb higher amounts of vapors in low concentrations compared to a commercial granular activated carbon especially appropriate for the removal of small concentrations of contaminants from gas streams (see Figure 12a) and monoliths prepared from different commercial ACFs (see Figure 12b).[127] Thus, Nomex-derived ACFMs are particularly suitable adsorbents for the retention of VOCs.

5.1.2. SO_2 Retention. As mentioned above (section 2), polyaramid-based carbonaceous materials show high contents of both oxygen and nitrogen, which suggests the presence of a high amount of functional groups. This is beneficial to SO_2 retention, as oxygen and nitrogen functionalities can act both as adsorption and as oxidation sites for SO_2.[128] Muñiz et al.[33] investigated the SO_2 retention performance of polyaramid-based ACFs. Both Nomex and Kevlar-derived ACFs showed high and similar SO_2 retention capacity. Their SO_2 retention capacity is comparable to that of commercial

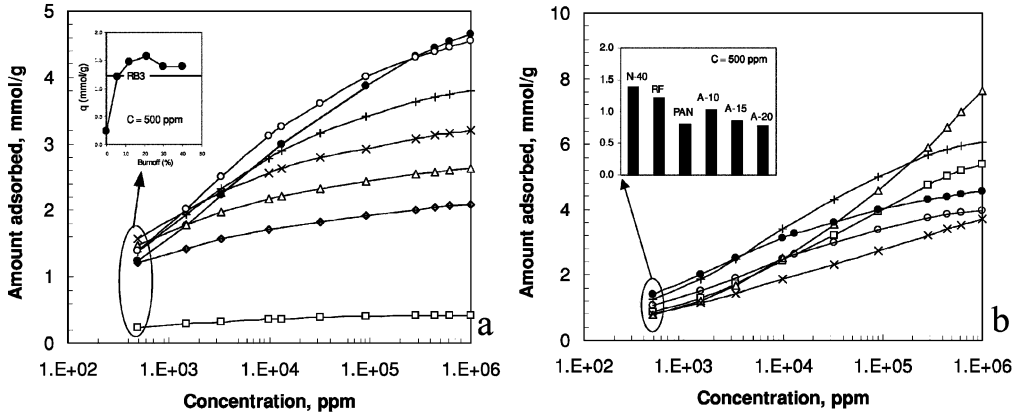

Figure 12. Adsorption isotherms of (a) *n*-butane at 30 °C on Nomex-based ACFMs activated to different BO degrees (□, 0%; △, 12%; × , 21%; +, 30%; ○, 40%) and on a pelletized activated carbon used as reference (●, Norit RB3); (b) *n*-butane at 30 °C on ACFMs prepared from various precursors: Nomex-based ACFM (40% BO) (●), PAN-based ACFM (×), phenolic resin-based ACFM (+), and pitch-based ACFM (○, A-10; □, A-15; △, A-20). Adapted from ref 127.

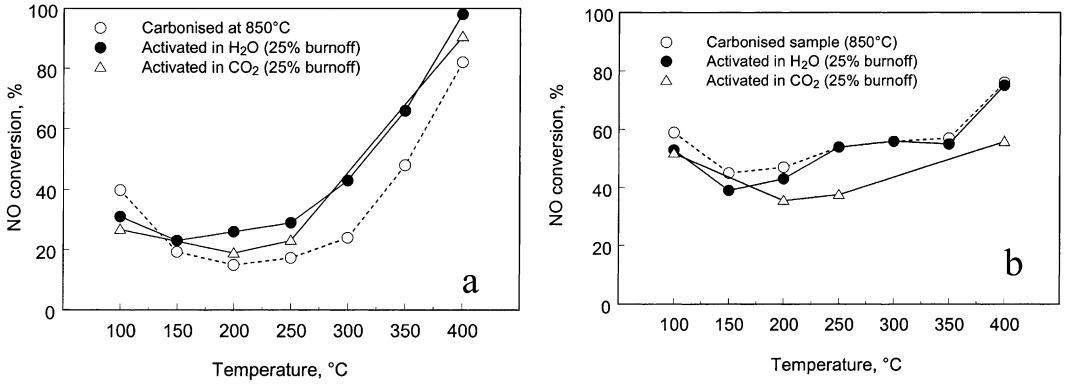

Figure 13. NO conversion as a function of temperature catalyzed by (a) Kevlar and (b) Nomex carbonized and activated with H_2O or CO_2. Adapted from ref 32.

PAN-derived ACFs, but the amount of SO_2 retained before the outlet SO_2 concentration reaches 5% of the inlet concentration, or *utilization degree*, is much higher. The basic character of the polyaramid-derived ACFs seemed to contribute greatly to their good performance. The corresponding carbon fiber-based monoliths[35] showed similar performance to that of the loose carbon fibers, but a lower utilization degree.

5.1.3. Selective Catalytic Reduction of NO_x. Selective catalytic reduction (SCR) is a recently developed technology to remove NO_x efficiently from the flue gas of combustion units. SCR catalysts enhance the reduction of NO_x in the presence of oxygen by ammonia, which is injected into the flue gases exhaust. The usual commercial scale process uses vanadium/titanium oxide catalysts, which exhibit high conversions between 300 and 400 °C. In this temperature range, the flue gases contain high concentrations of particulates and contaminants (SO_2, Ar, etc.) which shorten the life of the catalyst. Hence, there is a great interest in the development of SCR catalysts active at low temperatures.[129] Polyaramid-derived ACFs have been used both as catalysts and as catalyst supports in low-temperature SCR processes.

ACFs as Catalysts. As seen in section 2, carbonized polyaramid fibers show a high heteroatom content. This is expected to be beneficial in the reduction activity of the carbon catalyst toward NO,[130,131] as nitrogen functionalities enhance NO and O_2 adsorption on the carbon surface, and oxygen oxidizes NO to NO_2. Indeed, Muñiz et al.[32] confirmed the good performance of polyaramid-based carbon fibers for low-temperature SCR. Figure 13 shows the conversions obtained at different temperatures for NO reduction using Kevlar and Nomex fibers carbonized and activated with H_2O and CO_2. NO conversions in the range 40−80% were achieved with carbonized fibers at temperatures below 300 °C. Nomex-based carbon fibers showed higher catalytic activities than Kevlar-based ones, which was related to the higher basicity of the former (a surface density of basic groups of 775 μmol g^{-1} for carbonized Nomex and of 375 μmol g^{-1} for Kevlar were determined). No significant improvement in NO conversion was introduced by the activation of the carbonized fibers up to 25% BO, which suggested that the porosity created during activation was not involved in NO reduction, probably as a consequence of diffusion limitations. The ACFMs prepared by agglomeration of carbonized Nomex fibers with powdered phenolic resin and subsequent curing[35] showed similar performance to that of the loose carbon fibers.[32]

ACFs as Catalyst Supports. Several carbon-supported catalysts are known to be highly active toward NO_x reduction below 250 °C. One of the advantages of carbonaceous supports over inorganic supports is the possibility of controlling their textural properties by controlled gasification. Besides, as mentioned above, ACFs show a number of advantages over powdered and granulated carbons. Indeed, ACF supports have been proved to be more efficient than granulated active carbon or Al_2O_3 supports.[132] Marbán et

Table 3. CO_2, CH_4, O_2, and N_2 Kinetic Rate Constants and Selectivities for CO_2/CH_4 and O_2/N_2 Calculated with the LDF Model for the Pyrolyzed Material and Selected CMSs Prepared through CVD of Benzene (Bz) and Methane (Mt) on Nomex-Derived ACFs Activated to 21% BO[a]

	k/s^{-1}			k/s^{-1}		
	CO_2	CH_4	$k(CO_2)/k(CH_4)$	O_2	N_2	$k(O_2)/k(N_2)$
Takeda 3A	8.06×10^{-3}	4.56×10^{-4}	17.7	1.32×10^{-2}	9.76×10^{-4}	13.5
pyrolyzed	1.04×10^{-2}	3.77×10^{-4}	27.6	9.32×10^{-3}	4.41×10^{-3}	2.11
Bz 3-150	1.91×10^{-2}	0 ($t < 500$ s)[b]	∞[b]	6.62×10^{-3}	0 ($t < 50$ s)	∞[b]
Bz 3-180	9.10×10^{-3}	0 ($t < 600$ s)[b]	∞[b]	8.33×10^{-3}	0 ($t < 120$ s)	∞[b]
Bz 3-210	8.59×10^{-3}	0 ($t < 600$ s)[b]	∞[b]	8.59×10^{-3}	0 ($t < 120$ s)	∞[b]
Mt 100-20	3.8×10^{-3}	1.7×10^{-4}	22.4	3.1×10^{-3}	6.3×10^{-4}	4.9
Mt 100-30				6.8×10^{-4}	2.1×10^{-4}	3.2
Mt 23-45	5.9×10^{-3}	2.2×10^{-4}	26.8		4.1×10^{-3}	
Mt 23-60	3.0×10^{-3}	1.9×10^{-4}	15.8	$3.0 \times 10^{-}$	5.8×10^{-4}	5.2

[a] The first number indicates the concentration of the organic species in the gas flow, and the second is the CVD treatment time in minutes. The commercial carbon molecular sieve Takeda 3A is included for comparison. Adapted from refs 97 and 125. [b] Adsorption of CH_4 or N_2 is not detected at this time.

al.[133,134] have prepared Nomex rejects-based ACF composites-supported manganese oxides and studied their performance as low-temperature SCR catalysts. A low-density monolith made of carbonized Nomex rejects was fabricated and subjected to different surface-conditioning treatments to maximize the dispersion and loading of manganese oxides, which were highly active at 150 °C (NO_x conversion was close to 85%, and selectivity was above 95%). In a more complete study, the fabrication of fibrous monolith-supported catalysts to be used in low-temperature SCR of NO_x was optimized,[135] attempting to surpass the catalytic performance of the already highly active manganese oxide catalysts and to overcome deactivation by SO_2, which is one of the main drawbacks of the use of these catalysts under practical conditions. With this purpose, different carbon fibers were used as monolith supports (coal tar pitch-, Rayon-, PAN-, Nomex-, and phenolic resin-based fibers), and metal oxides other than manganese oxide (nickel, chromium, vanadium, and iron oxides) were used as catalysts. Iron oxide supported on a Nomex rejects-based ACF composite was selected as an optimal catalyst for the SCR process, there being a compromise between high catalytic performance and moderate deactivation by SO_2. Kinetic analysis and temperature-programmed desorption of NO were conducted on this catalyst in order to reveal mechanistic features of the low-temperature SCR reaction.[136]

5.2. Gas Separation. CMSs are nanoporous materials that provide molecular separations of gases from their mixtures on the basis of the different adsorption kinetics of the species involved. Besides, certain versatility can be introduced in the preparation process, enabling the optimization of the pore entrance size[5] and surface modification[52] to enhance the selectivity for specific target molecules. As a result of these attractive features, they have been considered as catalyst supports,[137] porous membranes,[138] and adsorbents for pressure-swing adsorption processes.[139] It has been predicted that CMSs with fibrous shape could be the best adsorbents for pressure-swing adsorption application[140] because of their rapid adsorption/desorption rate and large adsorption capacity. Nevertheless, earlier efforts on modifying the pore structure of ACFs to make them suitable for air separation have been only partially successful.[140,141]

In their pioneering work, Freeman et al.[28] proposed the use of Kevlar-derived ACFs to separate carbon dioxide from air. Chromatograms and CO_2 breakthrough curves showed that these materials behaved much better than a rayon-based one, but unfortunately that work was not continued. Nomex polymer shows higher carbonization yields than Kevlar (see section 1) and, more important, the derived ACFs possess smaller and more uniform pore sizes irrespective of the activation conditions (see section 4). For these features, Nomex-based ACFs have been proposed as promising precursors for CMSs.[30,39,40] Accordingly, Nomex-derived ACFs have been modified through CVD of benzene and methane and their porosity has been characterized as explained in section 4.4. The performance of the resulting materials for CO_2/CH_4 and O_2/N_2 (air) separations was tested by measuring the kinetics of adsorption of the corresponding gases.[97,125] Table 3 shows absolute adsorption rates and selectivities. Some of the materials prepared through CVD of benzene exhibited higher selectivity and adsorption capacity than a commercial CMS designed for air separation (Takeda 3A), constituting the first report on successful modification through CVD of benzene of ACFs to yield fibrous CMSs valid for such separation. CMSs useful for the less demanding CO_2/CH_4 separation have been also prepared using CVD both of benzene and of methane.

Gas storage is another significant emerging application of activated carbons.[142] As shown before (see Figure 9), simple physical activation of Nomex produces ACFs with high surface areas and micropore volumes, and with high yields when the activation is carried out using Nomex pre-impregnated with small amounts of phosphoric acid.[42] Therefore, Nomex-derived adsorbents are good candidates for use as adsorbents in gas storage systems.

5.3. Electrochemistry: Carbon Electrodes. As has been shown, the control of porosity (which is well-known to determine the properties of the electrode/ electrolyte interface for electrochemical applications) is especially effective for polyaramid-derived carbon fibers so that they constitute appropriate precursors for carbon electrodes. Moreover, the fibrous structure facilitates the preparation of consolidated forms, avoiding the use of a binding substance, which gives additional profit from the point of view of the manufacturing process.[143]

5.3.1. Lithium Rechargeable Batteries. Polyaramid fibers have several potential advantages as precursors for anodes. Thus, they do not require an oxidative stabilization step

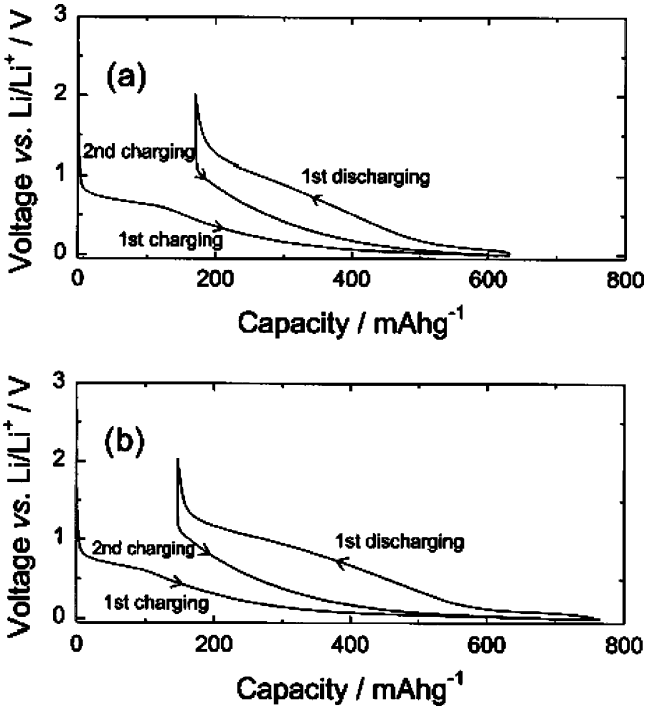

Figure 14. Galvanostatic charge/discharge voltage profiles of a Kevlar-derived carbon fiber prepared (a) in a single step and (b) in two steps with an intermediate heating at 410 °C. Adapted from ref 38.

previous to their carbonization, and the porous texture of polyaramid-based ACFs can be made large and restricted to very small pore sizes, which are expected to play a special role in intercalation and deintercalation of lithium ions within the microporous space of the anode. Therefore, Ko et al.[38] have tested the anodic performance of Kevlar-derived carbon fibers in lithium secondary batteries. Figure 14 shows the galvanostatic charge/discharge voltage profiles of Kevlar fibers subjected to single and two-step carbonization processes. Both carbons deliver a higher charging capacity than graphite (372 mAh g^{-1}) and exhibit the charge−discharge behavior usually observed in nongraphitizable carbons.[144] The results obtained are particularly good for the carbon fibers prepared with an intermediate heating step. In particular, their discharge capacity delivered near zero volts is notably high. Besides, their reversible capacity is higher than that of the fibers prepared by the one-step pyrolysis process. As explained in sections 2 and 4.5, the introduction of an intermediate isothermal step in the pyrolysis process leads to both higher carbon yields and higher amounts of micropores. The latter feature can justify the higher lithium insertion capacity of the fibers prepared by the two-step pyrolysis process.[145]

5.3.2. Double-Layer Capacitors. There is growing interest in the development of electrochemical energy storage systems under conditions in which the electrical power output is highly time-dependent (electrochemical supercapacitors).[146] Very recently, Leitner et al.[147] evaluated the performance of Nomex-derived ACFs as supercapacitors by cyclic voltammetry and impedance spectroscopy. Different types of ACF were tested: An ACF prepared by steam activation of pyrolyzed Nomex to 42% BO, which is designated as N-42 (see section 4.1);[39,40] an ACF prepared by physical activation with CO_2 to 76% BO (N-76); and two ACFs obtained by physical activation with CO_2 of Nomex pre-impregnated with different weight percentages of H_3PO_4 (see section 4.2),[42] designated as NP7-72 (7 wt %, 72% BO) and NP1-90 (1 wt %, 90% BO). As expected from their fibrous shape, all the ACFs were found to be easily processable to very mechanically stable electrodes. As Table 4 shows, the specific capacitance, *C*, improves with increasing BO/increasing S_{BET}. NP1-90 sample exhibits the best performance, behaving as an ideal capacitor with low internal resistance. On the other hand, N-42 showed diffusional barriers and a slightly higher resistance in the interior of the electrodes or the fibers themselves. The difference in behavior of these ACFs must be related to their different PSDs. Indeed, it has been established that activated carbons with larger percentage of bigger pores are more suitable to high-power supercapacitor applications because they can deliver more energy at a higher rate.[148] The results for Nomex-derived fibers are consistent with this fact, as wide micropores/small mesopores about 2−3 nm wide prevail in the material which performed better (NP1-90), whereas micropores <1 nm wide are dominant in the material which performed worse (N-42).

Table 4. Apparent BET Surface Area (S_{BET}) and Specific Capacitance (*C*) of Nomex-Based ACFs[a]

sample	S_{BET} (m^2 g^{-1})	*C* (F g^{-1})
N-42	1329	90
NP7-72	2408	150
N-76	2592	150
NP1-90	2832	175

[a] Nomenclature is defined on the text. Adapted from ref 147.

6. Conclusions and Prospects

The original expectations of Sing and co-workers have been confirmed by subsequent work: ACFs obtained from Kevlar and Nomex exhibit highly microporous textures that are not significantly widened by activation even at high BO degrees and are independent of the preparation method and experimental conditions used. These effects were already related by Sing et al. to the highly ordered precursor structure, which yields a denser, less defective char than those prepared from less crystalline precursors (e.g., PAN).

However, the achievement of a homogeneous pore size irrespective of BO degree is not only related to the crystallinity of the precursor. Thus, Nomex is less crystalline than Kevlar whereas Nomex-derived carbonaceous materials show narrower PSDs than Kevlar-derived ones. The extent of cross-linking has a clear effect on the char reactivity and the type of porous structure obtained. The higher extent of cross-linking in Nomex pyrolysis must account for the more homogeneous pore size in carbons prepared from this polymer. Indeed, a higher amount of micropores is observed for Kevlar-derived carbonaceous fibers when cross-linking is enhanced during their pyrolysis by introduction of intermediate isothermal steps.

The presence of highly reactive areas in Kevlar chars, where the gasification reaction occurs preferentially, would give rise to a wider porosity as the BO degree is increased, whereas in the case of Nomex chars the more homogeneous gasification allows a larger development of porosity without creation of wide pores taking place.

As a consequence of the structural order of Nomex and Kevlar chars, these materials undergo a densification during the course of gasification (activation), which is reflected in an increase in the degree of structural order (as measured by X-ray diffraction) in the resulting chars as the BO degree increases. This gasification-induced densification competes with the porosity widening that normally is produced with increasing BO, which limits the extent of porosity widening in comparison with chars from conventional precursors.

From the standpoint of practical applications, homogeneity in micropore size is the main advantage of polyaramid-derived ACFs. The relative insensitivity of pore size to the activation method, activating agent, and/or experimental conditions can be regarded as a drawback as it limits the possibilities to tailor the porosity. However, a certain control is possible, which allows two clearly distinct cases: ultra-high surface area, super-microporous carbons, and ultra-microporous carbon molecular sieves. The former have good prospects for use in gas and electric energy storage, applications that are practically unexplored. On the other hand, ultra-microporous ACFs obtained by benzene CVD have provided some of the best results reported to date for the highly demanding air fractionation. Besides, Nomex-derived ACFs are particularly appropriate adsorbents for VOCs at the small concentrations usually found in polluted environments, as they are much more microporous than conventional carbon adsorbents.

Besides porous texture, surface chemistry also plays a role in the applications of polyaramid-derived fibers as adsorbents for SO_2 retention and catalysts for selective reduction of NO_x. In the former case, oxygen and nitrogen functionalities can act as oxidation sites for SO_2; in the latter, nitrogen functionalities enhance NO and O_2 adsorption on the carbon surface and oxygen oxidizes NO to NO_2. The incorporation of nitrogen in the polyaromatic structures during pyrolysis yielding basic chars also contributes to their good performance as adsorbents for SO_2 retention and merits further study.

Overall, the polyaramids considered here yield carbon adsorbents with outstandingly homogeneous pore structures through simple and cost-effective approaches, thus constituting a competitive alternative in many applications to carbons of highly uniform porosity prepared by more elaborate and expensive approaches.

Acknowledgment. For several years, the authors have benefited from advice, support and polyaramid samples from Javier Fernández, Blanca Llorente, and Celina Blanco (DuPont Asturias), who are cordially thanked. Financial support from the Spanish and Asturian governments through several funded projects is gratefully acknowledged.

References

(1) Schüth, F., Sing, K. S. W., Weitkamp, J., Eds. *Handbook of Porous Solids*; Wiley-VCH: Weinheim, 2002.
(2) Davis, M. E. *Nature* **2002**, *417*, 813.
(3) Schüth, F.; Schmidt, W. *Adv. Mater.* **2002**, *14*, 629.
(4) Stein, A. *Adv. Mater.* **2003**, *15*, 763.
(5) Kyotani, T. *Carbon* **2000**, *38*, 269.
(6) Ryoo, R.; Joo, S. H.; Jun, S. *J. Phys. Chem. B* **1999**, *103*, 7743.
(7) Lee, J.; Yoon, S.; Hyeon, T.; Oh, S. M.; Kim, K. B. *Chem. Commun.* **1999**, 2177.
(8) Ryoo, R.; Joo, S. H.; Kruk, M.; Jaroniec, M. *Adv. Mater.* **2001**, *13*, 677.
(9) Joo, S. H.; Choi, S. J.; Oh, I.; Kwak, J.; Liu, Z.; Terasaki, O.; Ryoo, R. *Nature* **2001**, *412*, 169.
(10) Yang, H.; Shi, Q.; Liu, X.; Xie, S.; Jiang, D.; Zhang, F.; Yu, C.; Tu, B.; Zhao, D. *Chem. Commun.* **2002**, 2842.
(11) Ehrburger-Dolle, F.; Morfin, I.; Geissler, E.; Bley, F.; Livet, F.; Vix-Guterl, C.; Saadallah, S.; Parmentier, J.; Reda, M.; Patarin, J.; Iliescu, M.; Werckmann, J. *Langmuir* **2003**, *19*, 4303.
(12) Kruk, M.; Jaroniec, M.; Kim, T.-W.; Ryoo, R. *Chem. Mater.* **2003**, *15*, 2815.
(13) Kim, T.-W.; Park, L.-S.; Ryoo, R. *Angew. Chem., Int. Ed.* **2003**, *42*, 4375.
(14) Lu, A.; Kiefer, A.; Schmidt, W.; Schüth, F. *Chem. Mater.* **2004**, *16*, 100.
(15) Kim, C. H.; Lee, D.-K.; Pinnavaia, T. J. *Langmuir* **2004**, *20*, 5157.
(16) Xia, Y.; Mokaya, R. *Adv. Mater.* **2004**, *16*, 1553.
(17) Yang, C.-M.; Weidenthaler, C.; Spliethoff, B.; Mayanna, M.; Schüth, F. *Chem. Mater.* **2005**, *17*, 355.
(18) Chai, G. S.; Yoon, S. B.; Yu, J.-S.; Choi, J.-H.; Sung, Y.-E. *J. Phys. Chem. B* **2004**, *108*, 7074.
(19) Vinu, A.; Streb, C.; Murugesan, V.; Hartmann, M. *J. Phys. Chem. B* **2003**, *107*, 8297.
(20) Ma, Z.; Kyotani, T.; Tomita, A. *Chem. Commun.* **2000**, 2365.
(21) Ma, Z.; Kyotani, T.; Liu, Z.; Terasaki, O.; Tomita, A. *Chem. Mater.* **2001**, *13*, 4413.
(22) Gogotsi, Y.; Nikitin, A.; Ye, H.; Zhou, W.; Fischer, J. E.; Yi, B.; Foley, H. C.; Barsoum, M. W. *Nat. Mater.* **2003**, *2*, 591.
(23) Freeman, J. J.; Tomlinson, J. B.; Sing, K. S. W.; Theocharis, C. R. *Carbon* **1993**, *31*, 865.
(24) Tomlinson, J. B.; Freeman, J. J.; Sing, K. S. W.; Theocharis, C. R. *Carbon* **1995**, *33*, 789.
(25) Freeman, J. J.; Tomlinson, J. B.; Sing, K. S. W.; Theocharis, C. R. *Carbon* **1995**, *33*, 795.
(26) Pilato, L. A.; Michno, M. J. *Advanced Composite Materials*; Springer-Verlag: Berlin, 1994.
(27) Freeman, J. J.; Bhatia, G. S.; Gimblett, F. G. R.; Reynolds, A. J.; Sing, K. S. W. *Proceedings of 20th Biennal Carbon Conf.*, Santa Barbara, CA, 1991; p 98.
(28) Freeman, J. J.; Gimblett, F. G. R.; Hayes, R. A.; Amin, Z. M.; Sing, K. S. W. In *Characterization of Porous Solids II*; Rodríguez-Reinoso, F., Rouquerol, J., Sing, K. S. W., Unger, K. K., Eds.; Elsevier: Amsterdam, 1991; p 319.
(29) Yoon, S.-H.; Kim, B. C.; Korai, Y.; Mochida, I. *Proceedings of the 22nd Biennal Carbon Conf.*, San Diego, CA, 1995; p 218.
(30) Stoeckli, F.; Centeno, T. A.; Fuertes, A. B.; Muñiz, J. *Carbon* **1996**, *34*, 1201.
(31) Martínez-Alonso, A.; Jamond, M.; Montes-Morán, M. A.; Tascón, J. M. D. *Microporous Mater.* **1997**, *11*, 303.
(32) Muñiz, J.; Marbán, G.; Fuertes, A. B. *Appl. Catal. B* **1999**, *23*, 25.
(33) Muñiz, J.; Marbán, G.; Fuertes, A. B. *Environ. Prog.* **2000**, *19*, 246.
(34) Blanco López, M. C.; Martínez-Alonso, A.; Tascón, J. M. D. *Carbon* **2000**, *38*, 1177.
(35) Marbán, G.; Fuertes, A. B.; Nevskaia, D. M. *Carbon* **2000**, *38*, 2167.
(36) Blanco López, M. C.; Martínez-Alonso, A.; Tascón, J. M. D. *Microporous Mesoporous Mater.* **2000**, *34*, 171.
(37) Blanco López, M. C.; Villar-Rodil, S. M.; Martínez-Alonso, A.; Tascón, J. M. D. *Microporous Mesoporous Mater.* **2000**, *41*, 319.
(38) Ko, K. S.; Park, C. W.; Yoon, S.-H.; Oh. S. M. *Carbon* **2001**, *39*, 1619.
(39) Villar-Rodil, S.; Denoyel, R.; Rouquerol, J.; Martínez-Alonso, A.; Tascón, J. M. D. *Carbon* **2002**, *40*, 1369.
(40) Villar-Rodil, S.; Denoyel, R.; Rouquerol, J.; Martínez-Alonso, A.; Tascón, J. M. D. *J. Colloid Interface Sci.* **2002**, *252*, 169.
(41) Suárez-García, F.; Martínez-Alonso, A.; Tascón, J. M. D. *Fuel Process. Technol.* **2002**, *77*−*78*, 237.
(42) Suárez-García, F.; Paredes, J. I.; Martínez-Alonso, A.; Tascón, J. M. D. *J. Mater. Chem.* **2002**, *12*, 3213.
(43) Suárez-García, F.; Martínez-Alonso, A.; Tascón, J. M. D. *Carbon* **2004**, *42*, 1419.
(44) Suárez-García, F.; Martínez-Alonso, A.; Tascón, J. M. D. *Microporous Mesoporous Mater.* **2004**, *75*, 73.
(45) Krasnov, Y. P.; Savikov, V. M.; Sokolov, L. B.; Logunova, V. I.; Belyarov, V. K.; Polyakova, T. A. *Polym. Sci. USSR* **1966**, *8*, 380.
(46) Khanna, Y. P.; Pearce, E. M.; Smith, J. S.; Burkitt, D. T.; Njuguna, H.; Hinderlang, D. M.; Forman, B. D. *J. Polym. Sci., Polym. Chem.* **1981**, *19*, 2817.
(47) Brown, J. R.; Power, A. *J. Polym. Degrad. Stabil.* **1982**, *4*, 379.
(48) Schulten, H. R.; Plage, B.; Ohtani, H.; Tsuge, S. *Makrom. Chem.* **1987**, *155*, 1.
(49) Carroccio, S.; Puglisi, C.; Montaudo, G. *Macromol. Chem. Phys.* **1999**, *200*, 2345.
(50) Tomizuka, I.; Isoda, Y.; Amamiya, A. *Tanso* **1981**, *106*, 93.
(51) Fitzer, E.; Kompalik, D.; Kunz, M. In *Carbon'86 Proceedings*; DKG: Baden-Baden, Germany, 1986; p 847.
(52) Bansal, R. C.; Donnet, J.-B.; Stoeckli, F. *Active Carbon*; Marcel Dekker: New York, 1988.
(53) Mosquera, M. E. G.; Jamond, M.; Martínez-Alonso, A.; Tascón,. J. M. D. *Chem. Mater.* **1994**, *6*, 1918.
(54) Bourbigot, S.; Flambard, X.; Poutch, F. *Polym. Degrad. Stabil.* **2001**, *74*, 283.
(55) Villar-Rodil, S. M.; Martínez-Alonso, A.; Tascón, J. M. D. *J. Anal. Appl. Pyrol.* **2001**, *58*−*59*, 105.

(56) Villar-Rodil, S.; Paredes, J. I.; Martínez-Alonso, A.; Tascón, J. M. D. *Chem. Mater.* **2001**, *13*, 4297.
(57) Villar-Rodil, S., Paredes, J. I.; Martínez-Alonso, A.; Tascón, J. M. D. *J. Therm. Anal. Calorim.* **2002**, *70*, 37.
(58) Suárez-García, F.; Villar-Rodil, S.; Blanco, C. G.; Martínez-Alonso, A.; Tascón, J. M. D. *Chem. Mater.* **2004**, *16*, 2639.
(59) Fitzer, E., Köchling, K.-H., Boehm, H. P., Marsh, H. *Pure Appl. Chem.* **1995**, *67*, 473.
(60) Cuesta, A.; Martínez-Alonso, A.; Tascón, J. M. D.; Bradley, R. H. *Carbon* **1997**, *35*, 967.
(61) Cuesta, A. Ph.D. Thesis, University of Oviedo, 1994.
(62) García-Martínez, J.; Cazorla-Amorós, D.; Linares-Solano, A. *Stud. Surf. Sci. Catal.* **2000**, *128*, 485.
(63) Lozano-Castelló, D.; Cazorla-Amorós, D.; Linares-Solano, A. *Chem. Eng. Technol.* **2003**, *26*, 852.
(64) Lozano-Castelló, D.; Cazorla-Amorós, D.; Linares-Solano, A. *Carbon* **2004**, *42*, 1233.
(65) Villar-Rodil, S.; Martínez-Alonso, A.; Tascón, J. M. D. *J. Therm. Anal. Calorim.* **2005**, *79*, 529.
(66) Martínez-Alonso, A.; Tascón, J. M. D. In *Fundamental Issues in Control of Carbon Gasification Reactivity*; Lahaye, J., Ehrburger, P., Eds.; Kluwer: Dordrecht, 1991; p 435.
(67) Marsh, H.; Kuo, K. In *Introduction to Carbon Science*; Marsh, H., Ed.; Butterworths & Co.: London, 1989; p 107.
(68) Paredes, J. I.; Martínez-Alonso, A.; Tascón, J. M. D. *J. Microscopy* **2000**, *200*, 109.
(69) Bailey, A.; Maggs, F. A. P. British Patent No. 1,301,101, 1972.
(70) Ikegami, S.; Hirai, M.; Izumi, K. U.S Patent No. 4,362,646, 1982.
(71) Rodríguez-Reinoso, F.; Pastor, A. C.; Marsh, H.; Martínez, M. A. *Carbon* **2000**, *38*, 379.
(72) Sing, K. S. W. *Adv. Colloid Interface Sci.* **1998**, *76*−*77*, 3.
(73) Carrott, P. J. M.; Sing, K. W. S. In *Characterisation of Porous Solids, Studies in Surface Science and Catalysis, Vol. 39*; Unger, K. K., Rouquerol, J., Sing, K. S. W., Kral, H., Eds.; Elsevier: Amsterdam 1988; p 77.
(74) Suzuki, M. *Adsorption Engineering, Chemical Engineering Monographs*, Vol. 25; Kodansha and Elsevier: Tokyo and New York, 1990; p 31.
(75) Moyer, J. D.; Gaffney, T. R.; Armor, J. N.; Coe, C. G. *Microporous Mater.* **1994**, *2*, 229.
(76) Mariwala, R. K.; Acharya, M.; Foley, H. C. *Microporous Mesoporous Mater.* **1998**, *22*, 281.
(77) Hui, F.; Sassiat, P.; Sahraoui, Z.; Rosset, R. *Analusis* **1995**, *23*, 268.
(78) Kang, F. Y.; Huang, Z. H.; Liang, K. M.; Yang, J. B.; Wu, H. *Adsorpt. Sci. Technol.* **2001**, *19*, 423.
(79) Rouquerol, F.; Rouquerol, J.; Sing, K. S. W. *Adsorption by Powders & Porous Solids. Principles, Methodology and Applications*; Academic Press: London, 1999.
(80) Stoeckli, H. F.; Kraehenbuehl, F. *Carbon* **1981**, *19*, 353.
(81) Stoeckli, H. F.; Kraehenbuehl, F. *Carbon* **1984**, *22*, 297.
(82) Stoeckli, H. F.; Centeno, T. A. *Carbon* **1997**, *35*, 1097.
(83) Denoyel, R.; Fernandez-Colinas, J.; Grillet, Y.; Rouquerol, J. *Langmuir* **1993**, *9*, 515.
(84) González, M. T.; Sepúlveda-Escribano, A.; Molina-Sabio, M.; Rodríguez-Reinoso, F. *Langmuir* **1995**, *11*, 2151.
(85) Molina-Sabio, M.; González, M. T.; Rodríguez-Reinoso, F.; Sepúlveda-Escribano, A. *Carbon* **1996**, *34*, 505.
(86) Rodríguez-Reinoso, F.; Molina-Sabio, M.; González, M. T. *Langmuir* **1997**, *13*, 2354.
(87) Silvestre-Albero, J.; Gómez de Salazar, C.; Sepúlveda-Escribano, A.; Rodríguez-Reinoso, F. *Colloids Surf. A* **2001**, *187*−*188*, 151.
(88) Paredes, J. I.; Martínez-Alonso, A.; Tascón, J. M. D. *Microporous Mesoporous Mater.* **2003**, *65*, 93.
(89) Donnet, J. B.; Papirer, E.; Wang, W.; Stoeckli, H. F. *Carbon* **1994**, *32*, 183.
(90) Daley, M. A.; Tandon, D.; Economy, J.; Hippo, E. J. *Carbon* **1996**, *34*, 1991.
(91) Bóta, A.; László, K.; Nagy, L. G.; Copitzky, T. *Langmuir* **1997**, *13*, 6502.
(92) Vignal, V.; Morawski, A. W.; Konno, H.; Inagaki, M. *J. Mater. Res.* **1999**, *14*, 1102.
(93) Pfeifer, P.; Ehrburger-Dolle, F.; Rieker, T. P.; González, M. T.; Hoffman, W. P.; Molina-Sabio, M.; Rodríguez-Reinoso, F.; Schmidt, P. W.; Voss, D. J. *Phys. Rev. Lett.* **2002**, *88*, 115502.
(94) Shi, K.; Shiu, K.-K. *Anal. Chem.* **2002**, *74*, 879.
(95) Paredes, J. I.; Martínez-Alonso, A.; Tascón, J. M. D. *Langmuir* **2001**, *17*, 474.
(96) Paredes, J. I.; Villar-Rodil, S.; Martínez-Alonso, A.; Tascón, J. M. D. *J. Mater. Chem.* **2003**, *13*, 1513.
(97) Villar-Rodil, S.; Navarrete, R.; Denoyel, R.; Albiniak, A.; Paredes, J. I.; Martínez-Alonso, A.; Tascón, J. M. D. *Microporous. Mesoporous Mater.* **2005**, *77*, 109.
(98) Carrott, P. J. M.; Freeman, J. J. *Carbon* **1991**, *29*, 409.
(99) Garrido, J.; Linares-Solano, A.; Martín-Martínez, J. M.; Molina-Sabio, M.; Rodríguez-Reinoso, F.; Torregrosa, R. *Langmuir* **1987**, *3*, 76.
(100) Inagaki, M. *New Carbon Materials*; Elsevier: Amsterdam, 2000; p 130.
(101) Alcañiz-Monge, J.; Cazorla-Amorós, D.; Linares-Solano, A. *Fibras de Carbón: Preparación y Aplicaciones*; Univ. Alicante: Spain, 1998; p 109.
(102) Mangun, C. L.; Daley, M. A.; Braatz, R. D.; Economy, J. *Carbon* **1998**, *36*, 123.
(103) Ryu, Z. Y.; Zheng, J. T.; Wang, M. H.; Zhang, B. J. *J. Colloid Interface Sci.* **2000**, *230*, 312.
(104) Carrott, P. J. M.; Nabais, J. M. V.; Carrott, M. M. L. R.; Pajares, J. A. *Carbon* **2001**, *39*, 1543.
(105) Lee, Y. S.; Basova, Y. V.; Edie, D. D.; Reid, L. K.; Newcombe, S. R. *Carbon* **2003**, *41*, 2573.
(106) Qiao, W. M.; Yoon, S. H.; Korai, Y.; Mochida, I.; Inoue, S.; Sakurai, T.; Shimohara, T. *Carbon* **2004**, *42*, 1327.
(107) Tomkov, K.; Siemieniewska, T.; Czechowski, F.; Jankowska, A. *Fuel* **1977**, *56*, 121.
(108) Freeman, J. J.; Gimblett, F. G. R.; Roberts, A.; Sing, K. S. W. *Carbon* **1987**, *25*, 559.
(109) Wigmans, T. *Carbon* **1989**, *27*, 13.
(110) Ryu, S. K.; Jin, H.; Gondy, D.; Pusset, N.; Ehrburger, P. *Carbon* **1993**, *31*, 841.
(111) Villar-Rodil, S.; Martínez-Alonso, A.; Pajares, J. A.; Tascón, J. M. D.; Jasieńko-Hałat, M.; Broniek, E.; Kaczmarczyk, J.; Jankowska, A.; Albiniak, A.; Siemieniewska, T. *Microporous Mesoporous Mater.* **2003**, *64*, 11.
(112) Foster, K. L.; Fuerman, R. G.; Economy, J.; Larson, S. M.; Rood, M. J. *Chem. Mater.* **1992**, *4*, 1068.
(113) Magnun, C. L.; Daley, M. A.; Braatz, R. D.; Economy, J. *Carbon* **1998**, *36*, 123.
(114) Centeno, T. A.; Marbán, G.; Fuertes, A. B. *Carbon* **2003**, *41*, 843.
(115) Almazán-Almazán, M. C.; Fernández-Morales, I.; Domingo-García, M.; López- Garzón, F. J.; Pérez-Mendoza, M.; Suárez-García, F.; Martínez-Alonso, A.; Tascón, J. M. D. *Carbon 2004: Program and Abstracts*; Omnipress: Providence, RI, 2004; p 203.
(116) Domingo-García, F.; López-Garzón, F. J.; Moreno-Castilla, C.; Pyda, M. *J. Phys. Chem. B* **1997**, *101*, 8191.
(117) Jagtoyen, M.; Thwaites, M.; Stencel, J.; McEnaney, B.; Derbyshire, F. *Carbon* **1992**, *30*, 1089.
(118) Teng, H.; Yeh, T. S.; Hsu, L. Y. *Carbon* **1998**, *36*, 1387.
(119) Laine, J.; Calafat, A.; Labady, M. *Carbon* **1989**, *27*, 191.
(120) Molina-Sabio, M.; Rodríguez-Reinoso, F.; Caturla, F.; Sellés, M. J. *Carbon* **1995**, *33*, 1105.
(121) Jagtoyen, M.; Derbyshire, F. *Carbon* **1998**, *36*, 1085.
(122) Girgis, B. S.; El-Hendawy, A.-N. A. *Microporous Mesoporous Mater.* **2002**, *52*, 105.
(123) Suárez-García, F.; Martínez-Alonso, A.; Tascón, J. M. D. *J. Anal. Appl. Pyrol.* **2002**, *63*, 283.
(124) Villar-Rodil, S.; Martínez-Alonso, A.; Tascón, J. M. D. *J. Colloid Interface Sci.* **2002**, *254*, 414.
(125) Villar-Rodil, S.; Denoyel, R.; Rouquerol, J.; Martínez-Alonso, A.; Tascón, J. M. D. *Chem. Mater.* **2002**, *14*, 4328.
(126) Villar-Rodil, S.; Denoyel, R.; Rouquerol, J.; Martínez-Alonso, A.; Tascón, J. M. D. *Thermochim. Acta* **2004**, *420*, 141.
(127) Fuertes, A. B.; Marbán, G.; Nevskaia, D. M. *Carbon* **2003**, *41*, 87.
(128) Muñiz, J.; Herrero, J. E.; Fuertes, A. B. *Appl. Catal. B* **1998**, *18*, 171.
(129) Lowe, P. A. In *Environmental Catalysis, ACS Symposium Series 552*; Armor, J. N., Ed; American Chemical Society: Washington, 1994; p 205.
(130) Singoredjo, L.; Kapteijn, F.; Moulijn, J. A.; Martín-Martínez, J. M.; Boehm, H. P. *Carbon* **1993**, *31*, 213.
(131) Matzner, S.; Boehm, H. P. *Carbon* **1998**, *36*, 1697.
(132) Yosikawa, M.; Yasutake, A.; Mochida, I. *Appl. Catal. A* **1998**, *173*, 239.
(133) Marbán, G.; Fuertes, A. B. *Appl. Catal. B* **2001**, *34*, 43.
(134) Marbán, G.; Fuertes, A. B. *Appl. Catal. B* **2001**, *34*, 55.
(135) Marbán, G.; Antuña, R.; Fuertes, A. B. *Appl. Catal. B* **2003**, *41*, 323.
(136) Marbán, G.; Fuertes, A. B. *Catal. Lett.* **2002**, *84*, 1.
(137) Trimm, D. L.; Cooper, B. J. *J. Chem. Soc., Chem. Commun.* **1970**, 477.
(138) Ismail, A. F.; David, L. I. B. *J. Membr. Sci.* **2001**, *193*, 1.
(139) Jüntgen, H. *Carbon* **1977**, *15*, 273.
(140) Kawabuchi, Y.; Kishino, M.; Kawano, S.; Whitehurst, D. D.; Mochida, I. *Langmuir* **1996**, *12*, 4281.
(141) Kawabuchi, Y.; Sotowa, C.; Kishino, M.; Kawano, S.; Whitehurst, D. D.; Mochida, I. *Langmuir* **1997**, *13*, 2314.
(142) Derbyshire, F.; Jagtoyen, M.; Andrews, R.; Rao, A.; Martín-Gullón, I.; Grulke, E. A. In *Chemistry and Physics of Carbon, Vol. 27*; Radovic, L. R., Ed.; Marcel Dekker: New York, 2001; p 1.
(143) Frackowiak, E.; Béguin, F. *Carbon* **2001**, *39*, 937.
(144) Park, C. W.; Yoon, S.-H.; Lee, S. I.; Oh, S. M. *Carbon* **2000**, *38*, 995.
(145) Zheng, T.; Xing, W.; Dahn, J. R. *Carbon* **1996**, *34*, 1501.
(146) Conway, B. E. *Electrochemical Supercapacitors. Scientific Fundamentals and Technological Applications*; Kluwer Academic/Plenum Publishers: New York, 1999.
(147) Leitner, K.; Besenhard, J. O.; Lerf, A.; Villar-Rodil, S.; Suárez-García, F.; Martínez-Alonso, A.; Tascón, J. M. D. *J. Power Sources*, in press.
(148) Qu, D.; Shi, H. *J. Power Sources* **1998**, *74*, 99.

CM051339T